

University of Louisville

ThinkIR: The University of Louisville's Institutional Repository

Electronic Theses and Dissertations

5-2016

Efficacy of subcutaneous electrocardiogram leads for synchronous timing and aortic root cannulation for chronic counterpulsation therapy.

Stephen R. Carnahan
University of Louisville

Follow this and additional works at: <https://ir.library.louisville.edu/etd>



Part of the [Biomedical Engineering and Bioengineering Commons](#)

Recommended Citation

Carnahan, Stephen R., "Efficacy of subcutaneous electrocardiogram leads for synchronous timing and aortic root cannulation for chronic counterpulsation therapy." (2016). *Electronic Theses and Dissertations*. Paper 2358.

<https://doi.org/10.18297/etd/2358>

This Master's Thesis is brought to you for free and open access by ThinkIR: The University of Louisville's Institutional Repository. It has been accepted for inclusion in Electronic Theses and Dissertations by an authorized administrator of ThinkIR: The University of Louisville's Institutional Repository. This title appears here courtesy of the author, who has retained all other copyrights. For more information, please contact thinkir@louisville.edu.

EFFICACY OF SUBCUTANEOUS ELECTROCARDIOGRAM LEADS FOR
SYNCHRONOUS TIMING AND AORTIC ROOT CANNULATION FOR
CHRONIC COUNTERPULSATION THERAPY

By

Stephen R. Carnahan, B.S.
University of Louisville, 2016

A Thesis
Submitted to the Faculty of the
Speed School of Engineering of the University of Louisville
as Partial Fulfillment of the Requirements
for the Professional Degree

MASTER OF ENGINEERING

Department of Biomedical Engineering
University of Louisville
Louisville, Kentucky

May 2016

EFFICACY OF SUBCUTANEOUS ELECTROCARDIOGRAM LEADS FOR
SYNCHRONOUS TIMING AND AORTIC ROOT CANNULATION FOR
CHRONIC COUNTERPULSATION THERAPY

Submitted by:

Stephen R. Carnahan, BS

A Thesis Approved on

(DATE)

By the following Reading and Examination Committee

Guruprasad A. Giridharan, PhD, Thesis Director

Steven C. Koenig, PhD

Kevin G. Soucy, PhD

Peter M. Quesada, PhD

DEDICATION

This thesis is dedicated to my parents,

Mr. Mark S. Carnahan

and

Mrs. Tammy L. Carnahan

ACKNOWLEDGEMENTS

I would like to thank Dr. Mark Slaughter and Dr. Steven Koenig for allowing me the opportunity to join their research group in the fall of 2013. I would also like to thank Karen and Laura Lott for the countless hours of tutelage they have provided when I worked at CII as a co-op student. I am most grateful toward Dr. Gretel Monreal for always keeping me in high spirits and for Mr. Sobieski and Dr. Slaughter for giving me the opportunity to learn in the clinic and allowing me to find my career aspiration of practicing medicine. I am very appreciative of Dr. Guruprasad Giridharan for being an excellent mentor on this project and being exceedingly helpful through all of my road blocks. I could not have finished this project without him. I am also very appreciative toward Dr. Sean Warren for helping me with the MATLAB code used for ECG R-wave identification and comparison.

ABSTRACT

Background: Counterpulsation devices (CPD) require electrocardiogram (ECG) lead implantation for timing device filling and ejection with the native heart. Non-implantable leads limit the scope of CPD treatment to short-term therapy. Standard transvenous/epicardial ECG leads increase the invasiveness of therapy.

Methods: To overcome these limitations, subcutaneous ECG leads were tested in chronic (n=6) and acute (n=5) bovine models. ECG waveforms from clinical-grade epicardial (control) leads and subcutaneous (test) leads were simultaneously recorded resulting in 830 data epochs (30-s each) for a total of 44,614 heart beats. Device triggering using R-wave detection was calculated for each lead type and compared. Additionally, the hemodynamic benefits of CPD with aortic cannulation (n=5) was investigated during normal and pharmacologically-induced heart failure, hypertension, and hypotension test conditions.

Results: The subcutaneous leads provided 98.9% positive predictive value and 98.9% sensitivity compared to the epicardial ECG leads. Out of 40 subcutaneous leads implanted in chronic animals, lead migration (sensing-end movement >0.5cm, n=1) and lead fracture (n=1) were observed in two leads but did not adversely impact triggering efficacy due to lead redundancy. The CPD

cannulated to the aorta showed diminished left ventricular (LV) external work, LV end diastolic volume, and LV end systolic volume during 1:1 support compared to baseline in pharmacologically induced heart failure (HF). The CPD also augmented cardiac output, aortic mean pressure, aortic pulse pressure, and mean coronary artery flow.

Conclusion: These findings demonstrate the efficacy of chronic, subcutaneous ECG leads for CPD timing. The hemodynamic feasibility of the CPD cannulated to the aorta is equivalent or better than subclavian artery cannulation because of the proximity to the heart, which may increase the size of CPD patient population for warranted cases.

TABLE OF CONTENTS

Page

| | |
|----------------------------------------------|-----|
| TITLE PAGE..... | i |
| APPROVAL PAGE | iii |
| DEDICATION | iv |
| ACKNOWLEDGEMENTS..... | v |
| ABSTRACT | vi |
| LIST OF TABLES | ix |
| LIST OF FIGURES | x |
| I. BACKGROUND..... | 1 |
| II. CHRONIC <i>in-vivo</i> ANIMAL STUDY..... | 14 |
| A. INTRODUCTION..... | 14 |
| B. MATERIALS AND METHODS..... | 15 |
| C. RESULTS..... | 23 |
| D. DISCUSSION | 24 |
| III. ACUTE <i>in-vivo</i> ANIMAL STUDY..... | 27 |
| A. INTRODUCTION..... | 27 |
| B. MATERIALS AND METHODS..... | 28 |
| C. RESULTS..... | 30 |
| D. DISCUSSION..... | 41 |
| IV. CONCLUSION..... | 43 |
| V. LIST OF REFERENCES..... | 44 |
| VI. CURRICULUM VITAE..... | 48 |

LIST OF TABLES

Table 1. Summary of calves used for electrocardiogram (ECG) lead testing, lead migration testing, and damage testing.

Table 2. Positive predictive value (PPV) and sensitivity of R-wave detection calculated from subcutaneous ECG recordings. Each data epoch consists of 30 seconds of ECG signaling. Values are listed as mean \pm standard error.

Table 3. Summary of acute calves used for ECG lead testing and hemodynamic testing.

Table 4. Positive predictive value (PPV) and sensitivity of R-wave detection calculated from intra-operative subcutaneous ECG recordings. Each data epoch consists of 30 seconds of ECG signaling. Values are listed as mean \pm standard error.

Table 5. Hemodynamic parameters during acute counterpulsation therapy with the CPD device cannulated to the aorta in calves with pharmacologically induced hypertension, hypotension, and heart failure.

Table 6. Hemodynamic parameters during acute counterpulsation therapy with the CPD cannulated to carotid artery in calves with pharmacologically induced hypertension, hypotension, and heart failure [1].

LIST OF FIGURES

Figure 1. CPD sits in a Heart Failure (HF) patient's right side underneath the Pectoralis muscle via an infraclavicular incision. CPD is traditionally anastomosed to the right subclavian artery. The pump fills during systole and empties during diastole through a valveless ePTFE cannula [2].

Figure 2. Giridharan, et al. demonstrated equivalent or better hemodynamic benefits with the 30-ml CPD compared to 40-ml IABP. These pressure volume loops compare baseline heart failure (solid) to the 30-ml CPD with early filling late ejection (dashed) and late filling early ejection (dotted), and 40-ml IABP operating with early filling early ejection (dash-dot). These data indicate lower mean ejection LV Pressure (LVP) and external work (LVEW) with early filling late ejection algorithm compared with early filling early ejection and late filling early ejection algorithms [3].

Figure 3. Mean \pm standard error for hemodynamic parameters during baseline, counterpulsation device (CPD) support and intra-aortic balloon pump (IABP) support in a bovine animal study during pharmacologically induced hypertension, hypotension, and heart failure. LVEW, left ventricular external work; CAFd/LVEW, diastolic coronary artery flow normalized to left ventricular external work; LVO2 Consumption, left ventricular oxygen consumption during 1:1 support (IABP or CPD) normalized to baseline for that physiological condition [1].

Figure 4. Subcutaneous lead placement in bovine (left) and their analogous placement in humans (right) [4].

Figure 5. Photograph of first generation subcutaneous ECG leads fabricated by OSCOR and successfully tested in bovine model. The early lead design did not include tunneling needle and fixation tine, but demonstrated feasibility.

Figure 6. Photo of current ECG lead configuration complete with LEMO connector and strain relief (left) as well as tunneling needle (green arrow) and tine fixation (yellow arrow, upper right), and lead specifications (lower right).

Figure 7. Outline of the study.

Figure 8. Tunneling of the subcutaneous ECG lead (red arrow, upper left). Surgical staples (purple arrow) being placed for subcutaneous ECG lead fixation and to serve as a landmark for evaluating lead migration at necropsy (upper right). Aortic anastomosis (lower left) and location of ECG leads (white arrows, lower right).

Figure 9. Photograph of subcutaneous lead migration (red arrow) in a calf at the termination of the study. Staples were placed on the skin upon lead implantation

to be used as a reference for original lead placement. Only one lead was found to migrate more than 0.5cm as shown above.

Figure 10. Comparison of subcutaneous (dashed line) ECG demonstrated a 98.9% PPV and 98.9% sensitivity for counterpulsation timing compared to epicardial (solid line) ECG leads.

Figure 11. Pressure-volume loops obtained from an acute animal study at baseline (solid, no CPD support), and 1:1 CPD support (dashed) during a pharmacologically induced heart failure test condition. These PV loops demonstrate the reduction in LVEW, end systolic volume, and end diastolic volume with CPD support.

Figure 12. Aortic pressure (AoP, dotted), LV pressure (LVP, solid), and coronary artery flow waveforms obtained during a pharmacologically induced heart failure test condition at baseline (no CPD support), 1:2 support, and 1:1 support. These waveforms indicate a lower ventricular ejection pressure and higher aortic diastolic pressures (arrows, top) and coronary artery flow (arrows, bottom) during counterpulsation support.

Figure 13. Pressure-volume loops obtained at baseline (solid, no CPD support) and 1:1 CPD support (dashed) during a pharmacologically induced hypertension test condition. The hemodynamic benefits such as reductions in LVEW, end systolic volume, and end diastolic volume are not evident compared to the heart failure test condition as the stroke volume of the native heart (135 ml) was much greater than the counterpulsation device volume (30 ml).

Figure 14. Aortic pressure (AoP, dotted), LV pressure (LVP, solid), and coronary artery flow waveforms obtained during a pharmacologically induced hypertension test condition at baseline (no CPD support), 1:2 support, and 1:1 support. The hemodynamic benefits such as lower ventricular ejection pressure and higher aortic diastolic pressures (arrows, top) and coronary artery flow (arrows, bottom) are not evident compared to the heart failure test condition as the stroke volume of the native heart (135 ml) was much greater than the counterpulsation device volume (30 ml).

Figure 15. Pressure-volume loops obtained at baseline (solid, no CPD support), and 1:1 CPD support (dashed) during a pharmacologically induced hypotension test condition. The hemodynamic benefits such as reductions in LVEW, end systolic volume, and end diastolic volume are not evident compared to the heart failure test condition as the stroke volume of the native heart (82 ml) was much greater than the counterpulsation device volume (30 ml).

Figure 16. Aortic pressure (AoP, dotted), LV pressure (LVP, solid), and coronary artery flow waveforms obtained during a pharmacologically induced hypotension test condition at baseline (no CPD support), 1:2 support, and 1:1 support. These

waveforms indicate a lower ventricular ejection pressure and higher aortic diastolic pressures (arrows, top) and coronary artery flow (arrows, bottom) during counterpulsation support.

Figure 17. Pressure-volume loops at baseline (solid, no CPD support), and 1:1 CPD support (dashed) during a normal test condition. The hemodynamic benefits such as reductions in LVEW, end systolic volume, and end diastolic volume are not evident compared to the heart failure test condition as the stroke volume of the native heart (128 ml) was much greater than the counterpulsation device volume (30 ml).

Figure 18. Aortic pressure (AoP, dotted), LV pressure (LVP, solid), and coronary artery flow waveforms obtained during a normal test condition at baseline (no CPD support), 1:2 support, and 1:1 support. Lower ventricular ejection pressure and higher aortic diastolic pressures (arrows, top) and coronary artery flow (arrows, bottom) during counterpulsation support are not as evident compared to the heart failure test condition as the stroke volume of the native heart (135 ml) was much greater than the counterpulsation device volume (30 ml).

CHAPTER I - BACKGROUND

Heart Failure

Heart Failure (HF) is an incurable, progressive disease that afflicts 5,100,000 people in the United States with a 50% mortality rate within 5 years. According to the Center for Disease Control and Prevention, HF costs the nation \$32 billion per year including the cost of medication, medical services, and missed days of work for HF patients. The prevalence of heart failure continues to rise worldwide (~1,000,000 new patients per year) as the causes for heart failure such as obesity, coronary artery disease, and hypertension persist [5].

Currently, pharmacological agents including using beta blockers, diuretics, and ACE inhibitors is the preferred treatment option for HF patients until HF progresses to an extent that a more aggressive therapy such as heart transplantation or mechanical assist device therapy is warranted. Even though the US averaged \$8,915 per person on health care in 2012, the favorable outcomes for HF patients are low [6]. Muntwyler J, and colleagues reported one year mortality rates were 7.1%, 15.0%, and 28.0% for NYHA Class II, III, and IV, respectively [7]. Approximately 30% mortality was reported at two years post diagnosis in the RALES trial [8]. To combat this poor prognosis, heart transplantation has been used in conjunction with immunosuppressant drugs and

is considered the best form of end-stage HF therapy for long-term survival. However, the supply of donor hearts (~2,300/year in the US) remains relatively low while the demand continuously rises [9, 10].

Due to the shortage of available donor organs, alternative therapies such as mechanical circulatory support (MCS) device implantation are needed. This clinical need has led to significant research and development of cardiac assist devices for destination therapy (support until death) and bridge to transplant therapy (support until organ transplantation is available). Currently, for every donor heart successfully transplanted, approximately two MCS devices are placed in HF patients. The average cost of left ventricular assist devices is \$67,085 [11], which limits the use of these devices in developing countries. In order to expand the patient population for MCS therapy, a significant reduction in cost as well as risks associated with surgical implantation is required. Current chronic MCS devices require invasive surgical procedures (thoracotomies or sternotomies) and the use of Cardiopulmonary Bypass. These procedures involve risks of infection and other post-operative complications such as stroke and device thrombosis. Therefore, countries worldwide are slow to adopt MCS therapy as a means of HF treatment [12].

Intra-Aortic Balloon Pump

Moulopoulos, et al. developed a prototype of an Intra-Aortic Balloon Pump (IABP) in 1962. This device paved the way for counterpulsation as a means of MCS therapy that is cost-effective (\$800) [13]. Worldwide, IABP is implanted in over 160,000 patients per year and is effective in the treatment of cardiogenic shock and acute heart failure [14, 15]. IABP is a balloon which is surgically inserted into the descending aorta via access of the femoral artery using a modified Seldinger's technique. Counterpulsation therapy is attained by rapidly inflating the IABP immediately after the diastolic notch and quickly deflating the balloon just prior to ventricular systole.

The rapid inflation of the balloon increases the aortic diastolic pressure which improves end-organ perfusion and coronary perfusion (up to 100%) [16-21]. IABP deflation prior to ventricular systole decreases the ejection pressure of the native ventricle, reducing after-load and left ventricular external work (LVEW) [16, 22, 23]. The LV peak systolic pressure is reduced by up to 15% and the LV end diastolic pressure is reduced by approximately 30% [16, 19, 24]. Among other benefits is an increase in cardiac output and stroke volume, a decrease in heart rate, more efficient metabolic function, and improved end organ perfusion and function [25, 26]. IABP implantation is less invasive and consequently has fewer intra- and post-operative complications compared to ventricular assist devices. It cannot be used for chronic therapy and disallows ambulatory care for

patients receiving treatment. There is a critical clinical need to develop counterpulsation therapy for chronic and ambulatory use [19, 20, 22, 23, 27].

Synchronous Counterpulsation Devices

A number of devices have been developed to provide chronic counterpulsation including C-Pulse (Sunshine Medical, Eden Prairie MN), CardioVAD (LVAD Technologies, Detroit MI), and Symphony (Abiomed Inc., Danvers, MA) [28]. The C-Pulse is a non-blood contacting cuff that is implanted around the ascending aorta. The CardioVAD is a blood-contacting polyurethane sac that replaces a portion of the descending aorta. Both of these devices require the use of thoracotomies and cardiopulmonary bypass for implantation. Because LVAD Technologies and Sunshine Medical removed the minimally invasive quality of IABP when designing CardioPlus and Sunshine Heart, these devices now compete against other invasive MCS devices and have not been widely accepted clinically. However, Jeevanandam et al. have demonstrated the clinical benefits of the CardioPlus device such as increased cardiac output and end organ perfusion [28, 29]. Symphony is a 32 ml device that is implanted in the right subcutaneous pocket and anastomosed to the subclavian artery

CPD

A novel counterpulsation device was developed by SCR Inc. (Louisville, KY) in partnership with researchers at the University of Louisville [10]. This device is currently undergoing pre-clinical trials[4]. It consists of a 30-ml chamber, driveline, and outflow graft. The 30-ml chamber has a blood side and air side that is separated by a membrane. The 30-ml chamber sits in the pacemaker pocket of the right chest (figure 1). The driveline exits near the bottom right side of the thoracic cavity. The outflow graft made of ePTFE was designed to connect the 30-ml chamber to the right subclavian artery [3, 30]. The device is pneumatically driven. Air is pumped in between the outer hard shell and the inner membrane causing CPD ejection. This air is evacuated from the CPD chamber during CPD filling. In contrast to IABP, the CPD fills during ventricular systole and empties blood during diastole.

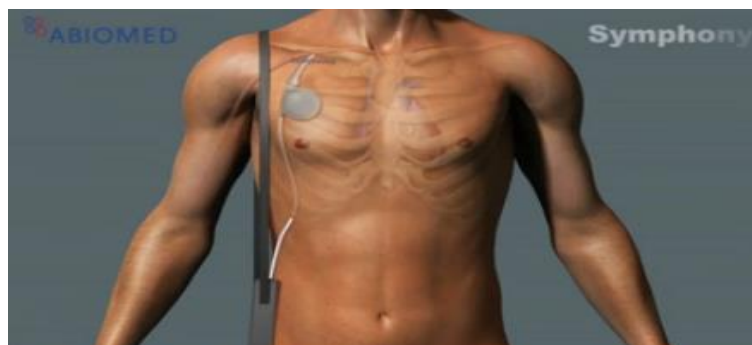


Figure 1. CPD sits in a HF patient's right side underneath the Pectoralis muscle via an infraclavicular incision. CPD is surgically anastomosed to the right subclavian artery. The pump fills during systole and empties during diastole through a valveless ePTFE cannula [2].

Giridharan, et al. demonstrated equivalent or better hemodynamic benefits with the CPD compared to 40-ml IABP in a computer simulation model of the human circulatory system (Figure 2) [3]. Bartoli, et al. demonstrated a reduction in LV oxygen consumption with the CPD compared to 40-ml IABP in a bovine model (Figure 3). In addition to better hemodynamic benefits, the CPD implantation is less invasive as it can be implanted in the right pacemaker pocket without the need to access the thoracic cavity of the patient. Importantly, it has the potential for chronic and ambulatory therapy as the device can be driven by a portable pneumatic driver weighing ~5 lbs. A significant distinction between an IABP and the CPD is that the IABP displaces blood in the native aorta while the CPD moves blood in and out of the subclavian artery. This enables the ejection and filling phases of the CPD to be longer than the balloon inflation and deflation phases of the IABP. Faster balloon deflation is required in IABP to prevent obstruction of the aorta during ventricular systole. This rapid deflation leads to reverse coronary flow which diminishes myocardial perfusion augmentation and hemodynamic benefits provided by the IABP.

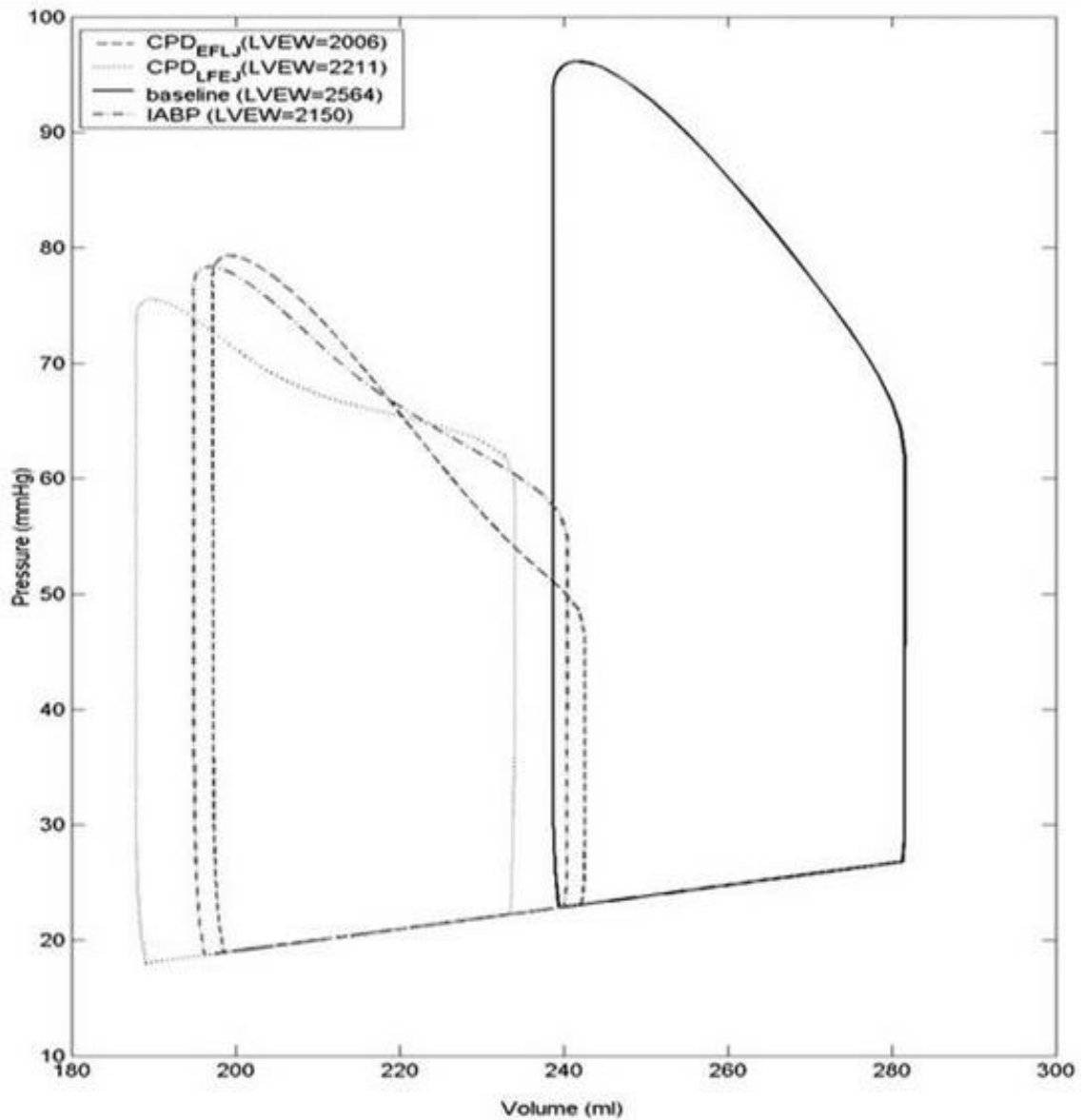


Figure 2. Giridharan, et al. demonstrated equivalent or better hemodynamic benefits with the 30-ml CPD compared to 40-ml IABP. These pressure volume loops compare baseline heart failure (solid) to the 30-ml CPD with early filling late ejection (dashed) and late filling early ejection (dotted), and 40-ml IABP operating with early filling early ejection (dash-dot). These data indicate lower mean ejection LV Pressure (LVP) and external work (LVEW) with early filling late ejection algorithm compared with early filling early ejection and late filling early ejection algorithms [3].

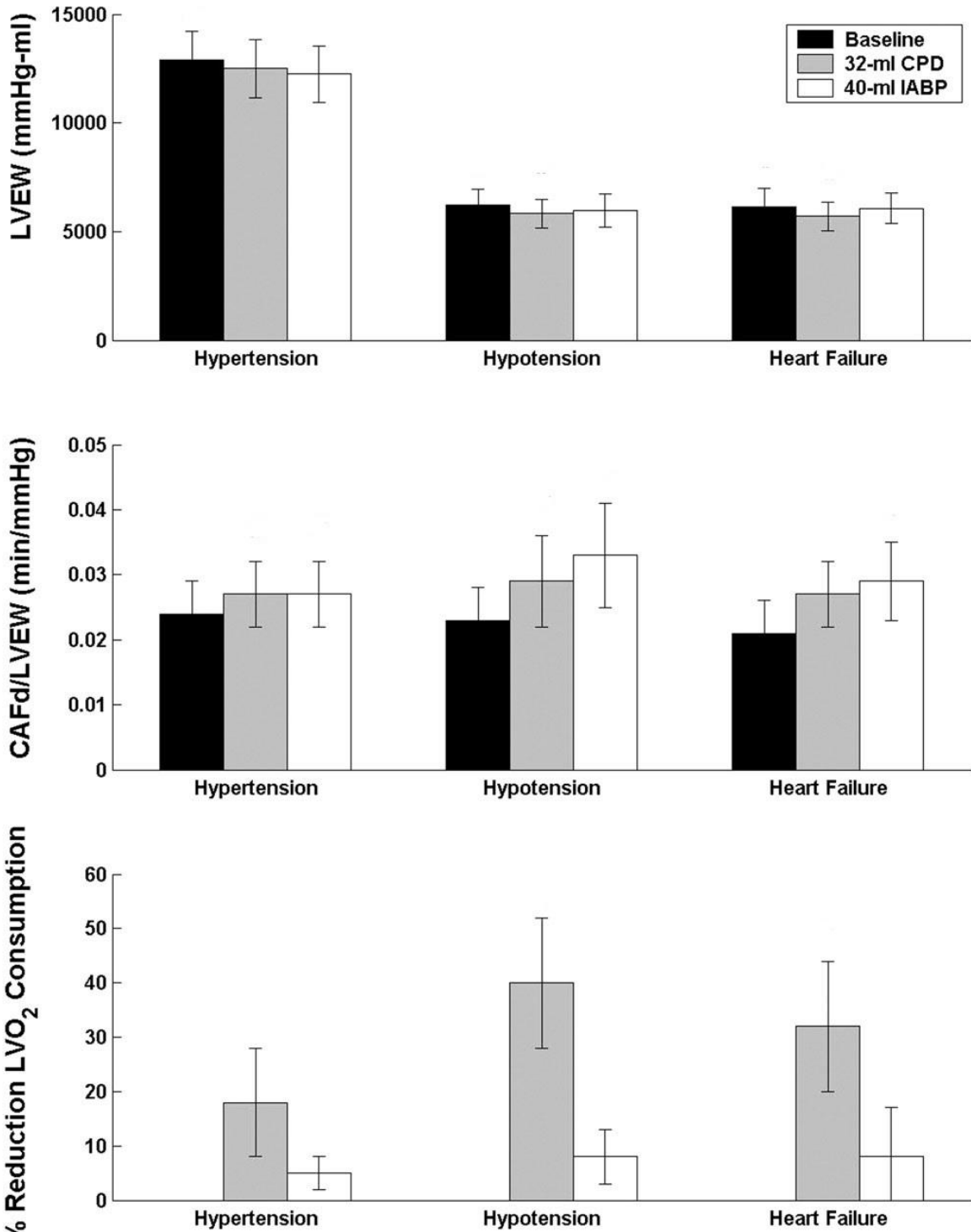


Figure 3. Mean \pm standard error for hemodynamic parameters during baseline, counterpulsation device (CPD) support and intra-aortic balloon pump (IABP) support in a bovine animal study during pharmacologically induced hypertension, hypotension, and heart failure. LVEW, left ventricular external work; CAFd/LVEW, diastolic coronary artery flow normalized to left ventricular external work; LVO₂ Consumption, left ventricular oxygen consumption during 1:1 support (IABP or CPD) normalized to baseline for that physiological condition [1].

CPD Anastomosis

CPD was originally developed to be anastomosed to a subclavian artery that has a minimum diameter of 8 mm. CPD implantation is contraindicated for patients with subclavian artery diameters of less than 8 mm as it cannot fully fill and eject, leading to blood stasis and device thrombosis. The subclavian artery size limits the number of patients that could benefit from CPD therapy [24, 25]. Therefore, as an alternative to the subclavian artery graft site, an aortic cannula was developed to expand the patient population to individuals with a small subclavian artery. Demonstrating the feasibility of the aortic anastomosis is one of the main objectives of this thesis (see CHAPTER 3).

ECG Acquisition

ECG signal is required to time CPD filling and ejection. Epicardial ECG leads increase the complexity of surgical implant and the risks of infection and/or micro-shocks. In order to remove these unwanted risks, an alternative approach is required to acquire ECG data while retaining signal fidelity. If the measured ECG signal is not adequate or if the CPD is not synchronized with the native heart, the CPD may increase ventricular workload and diminish myocardial perfusion. Therefore, it is important to find a long-term, reliable solution to accurately trigger the CPD.

Besides the use of epicardial leads, other forms of ECG monitoring have been considered for CPD [31]. For short-term devices such as IABP, surface electrodes (3- to 12-lead configuration) are often used, but these leads may be a significant clinical challenge due to motion artifacts and frequent need to replace surface electrodes, especially in ambulatory patients [32]. Alternatively, leads can be placed intravenously into the coronary sinus, which requires fluoroscopy and introduces additional risks to the patient (dislodgment, fracture, thrombosis, and infection) [15, 33, 34]. To overcome the limitations of current approaches, an alternative subcutaneous lead system was developed.

Subcutaneous ECG Lead Development

Subcutaneous ECG leads were developed to provide high-quality signal, and remove some of the negative effects of more invasive monitoring systems [35-37]. Subcutaneous refers to the area of lead implantation right beneath the skin. When joined with devices that reside in the pacemaker pocket of the right chest, subcutaneous lead placement over the right chest as shown in Figure 4 provides adequate spacing to detect the ECG [30].

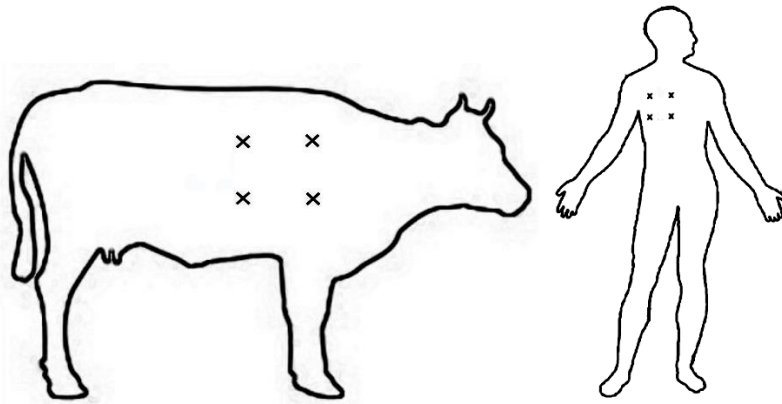


Figure 4. Subcutaneous lead placement in bovine (left) and their analogous placement in humans (right) [4].

SCR, Inc. completed the engineering development for integrated subcutaneous ECG leads, which consisted of two generations of development as shown in Figures 5-6. Fabrication was completed by OSCOR (Palm Harbor, FL). The current subcutaneous ECG lead configuration consists of four individual leads integrated into a single, electrically isolated cable. Each lead has a transducer on its distal end (ECG sensing) and a single connector on the proximal end that is attached to a signal conditioning and processing module that generates an ECG waveform used to trigger and control the CPD. Each lead uses a tine for fixation and a 1-cm exposed, non-insulated section for sensing cardiac electric potential. Each of the four sensors is on a 25cm length lead to provide maximum flexibility and separation distance of up to 50cm between a pair of sensors. A separation of 15 cm enables detection of a voltage differential (ECG) between paired sensors. The second group of four sensors provides a back-up ECG signal in the unexpected event of lead migration or fracture in two of the four leads of the first. Each group of four sensing leads are packaged into

a single silicone coated cable and integrated into a four-pin LEMO male connector (PEI-Genesis), which is mated to a female receptor for ECG signal conditioning and processing. The LEMO connectors have a threaded enclosure as well as an extended end to provide strain-relief [32, 38].



Figure 5. Photograph of first generation subcutaneous ECG leads fabricated by OSCOR and successfully tested in bovine model. The early lead design did not include tunneling needle and fixation tine, but demonstrated feasibility.

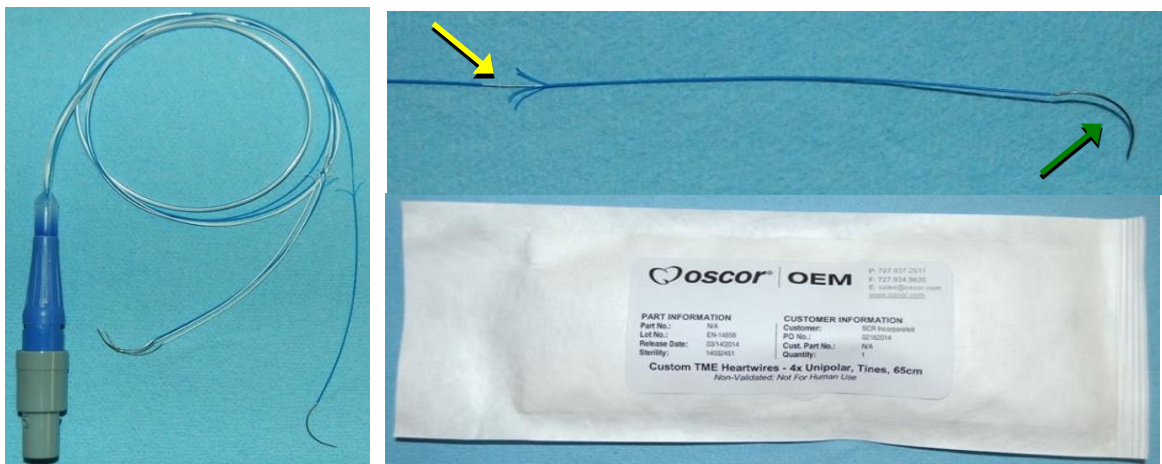


Figure 6. Photo of current ECG lead configuration complete with LEMO connector and strain relief (left) as well as tunneling needle (green arrow) and tine fixation (yellow arrow, upper right), and lead specifications (lower right).

Warren, et al. tested the performance of the previous generation subcutaneous lead system (6 bi-polar leads) in *in-vivo* animal experiments and found the subcutaneous leads to provide accurate and reliable R-wave detection as well as minimal lead migration, damage, and infection [4]. The lead has been redesigned to be unipolar and the lead configuration has been simplified to 4 leads. The primary objective of this thesis was to test the new lead design and configuration in acute bovine and chronic IHF bovine models. A secondary objective of the thesis was to demonstrate the hemodynamic feasibility of aortic cannulation of the CPD. The experimental design is shown in Figure 7.

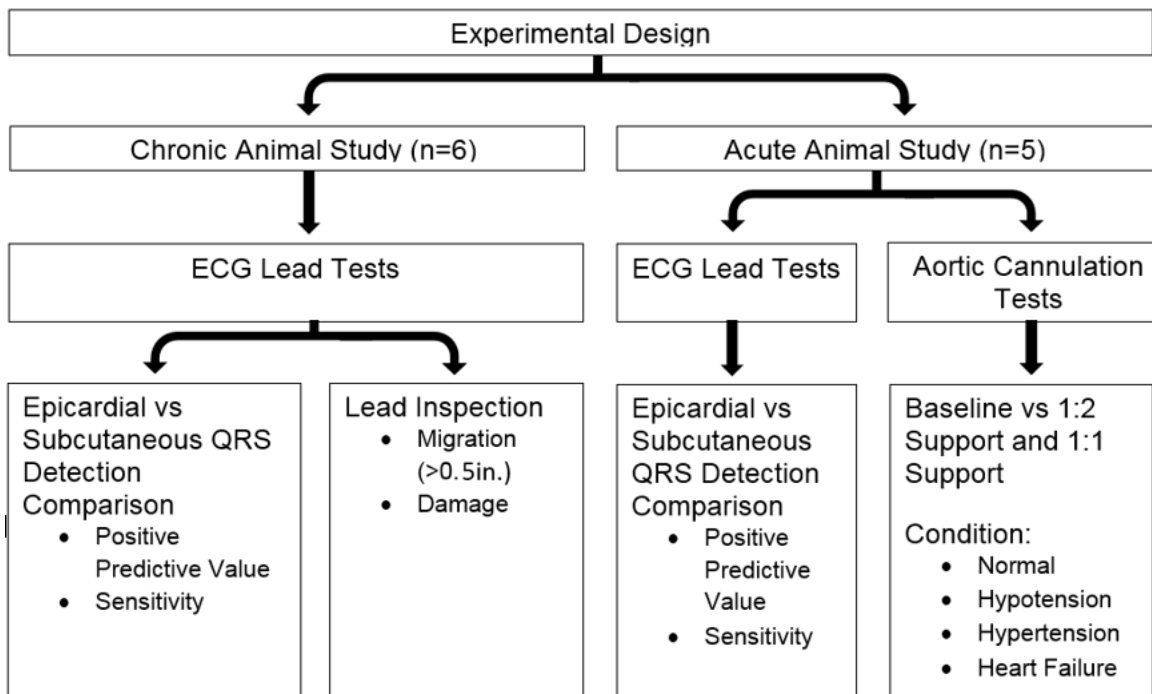


Figure 7. Experimental outline of the acute and chronic animal studies.

CHAPTER 2 – CHRONIC *in-vivo* ANIMAL STUDY

INTRODUCTION

The objectives of this study were to 1) demonstrate chronic subcutaneous lead efficacy in providing reliable cardiac signaling for proper device triggering and 2) quantify the amount of lead migration or other adverse events in long-term implantable subcutaneous ECG leads in a chronic ischemic heart failure (IHF) model. The study outline is shown in Table 1. Calves first underwent ischemic heart failure (IHF) induction procedures (n=6). IHF calves and control (non-IHF animal, n=1) were allowed to rest for 45 to 90 days in order to mature into a state of advanced heart failure. Next, CPD and ECG lead implantation was performed. ECG waveforms were collected using both epicardial and subcutaneous leads. At the end of each experiment, calves were euthanized. If a calf died before data could be acquired, then that calf was not averaged into the results.

A bovine model was selected because the anatomy of the heart and vasculature is similar to that of humans and bovine are more docile compared to porcine or ovine models when using devices with many externalized components. All animals used were cared for in accordance with the University of Louisville (UofL) Animal Care Committee and National Institutes of Health (NIH) guidelines.

Experimental procedures were approved by the UofL Institutional Animal Care and Usage Committee (IACUC).

| Animal ID | Length of Study | Procedure Date | Necropsy Date | Termination Reason |
|-----------|-----------------|----------------|---------------|----------------------------------------------|
| 1 | 1 day | 1/30/14 | 1/30/14 | died during surgery |
| 2 | 10 days | 5/12/14 | 5/20/14 | died early from heart failure |
| 3 | 30 days | 9/30/14 | 10/30/14 | full term |
| 4 | 30 days | 9/10/14 | 10/10/14 | full term |
| 5 | 10 days | 11/20/14 | 11/30/14 | euthanized early for pain management reasons |
| 6 | 31 days | 1/8/15 | 2/9/15 | full term |

Table 1. Summary of electrocardiogram (ECG) lead efficacy and lead migration testing in a bovine model of ischemic heart failure implanted with a CPD anastomosed to the aorta.

MATERIALS AND METHODS

IHF Induction Procedure

In a bovine model, IHF was induced (n=5) along with a control (non-IHF, n=1) for preparation of CPD implantation. Male Jersey calves (Oak Hill Genetics, Ewing, IL) weighing 60 kg on arrival from vendor were first quarantined for 14 days and treated with preventative medicine: Panacur (10mg/kg S.Q.), Marquis Paste (20mg/kg, P.O.), Iron Dextran (2.0ml I.M.), Ivomec (1ml/50ky S.Q.), and Excenel (2.2mg/kg S.Q.). After passing quarantine, calves underwent cardiac catheterization and IHF induction procedures using a target dose of polystyrene embolization solution (1.3% 90µm microsphere solution). This solution was mixed with equal amounts of saline and administered at a dose of 0.17 ml per kilogram of body weight.

For IHF induction procedures, food and water was withheld for 20 hours before surgery and the calves were given a Fentanyl transdermal patch for analgesia. At the time of surgery, general anesthesia was administered with Ketamine 4mg/kg and Valium 0.4mg/kg intravenously (IV) and later with Isoflurane. External ECG leads were sutured to the calves for ECG monitoring and pulse oximeters were used for intra-operative diagnostics. The following drugs and fluids were used as necessary under the control of an anesthesiologist to provide intraoperative support to the animal: Amiodarone, Lidocaine, Dobutamine, Phenylepinephrine, Lactated Ringers Solution, Vitamin B Complex Solution, Magnesium Sulfate, and Potassium Chloride. Every stage of the procedure was carried out aseptically. A 3-4cm incision was made in the jugular furrow. An Access™ Vascular Access Port (VAP) was inserted into the jugular vein. The VAP was tested for patency, flushed with 10ml saline, and locked with taurolidine-citrate catheter solution. The VAP port was placed into the pocket and secured to the muscle with 2-0 Vicryl sutures. An arteriotomy was performed and a catheter was placed in the carotid artery and secured. Patency was achieved and the catheter was connected to a pressure transducer line for intra-operative monitoring. A cordis sheath was placed into the carotid artery using the modified Seldinger's technique. Upon cardiac catheterization, spheres 90 microns in diameter were injected down the left anterior descending and circumflex coronary arteries of the calf to induce heart failure. Upon completion of the embolization procedure, the cordis sheath was removed and the arteriotomy was closed. The calves were then transferred to post-operative care for a period

of 45 to 90 days in order to mature into a state of advanced heart failure. Once heart failure was diagnosed by an ejection fraction of less than 35% the calves underwent a CPD implant procedure.

CPD, Subcutaneous, and Epicardial Lead Implant Procedure

The CPD implant procedure was similar to the embolization procedure in terms of pharmaceutical use, vascular access, and the steps taken for intra-operative monitoring. However, Succinylcholine (30mg) was given before the implant and a 25 cm incision was made over the 5th rib. The 5th rib was then removed and two rib retractors were used for exposure. Blunt dissection and electrical cautery were used to expose the aorta. Two groups of eight subcutaneous ECG electrodes were tunneled in four quadrants surrounding the chest incision and connected to the device externally. To track lead migration, the leads were secured beneath the cutaneous layer using surgical staples which were used as a placement reference (Figure 8). Three standard epicardial leads (Medtronic, 5071 Screw-In Leads 53 cm long) were also implanted into the epicardium for future waveform comparison [15]. Heparin was given to maintain an ACT above 250 seconds. The outflow/inflow graft was cut to ideal anatomic length. The aorta was partially clamped, an aortotomy was made, and the CPD graft was anastomosed using 3-0 Prolene suture. Hemostasis was checked and the graft was de-aired and connected to the CPD device. A 24mm flow probe was

placed on the outflow graft and tunneled out next to the driveline for post-operative monitoring. A chest tube was inserted and secured for drainage.

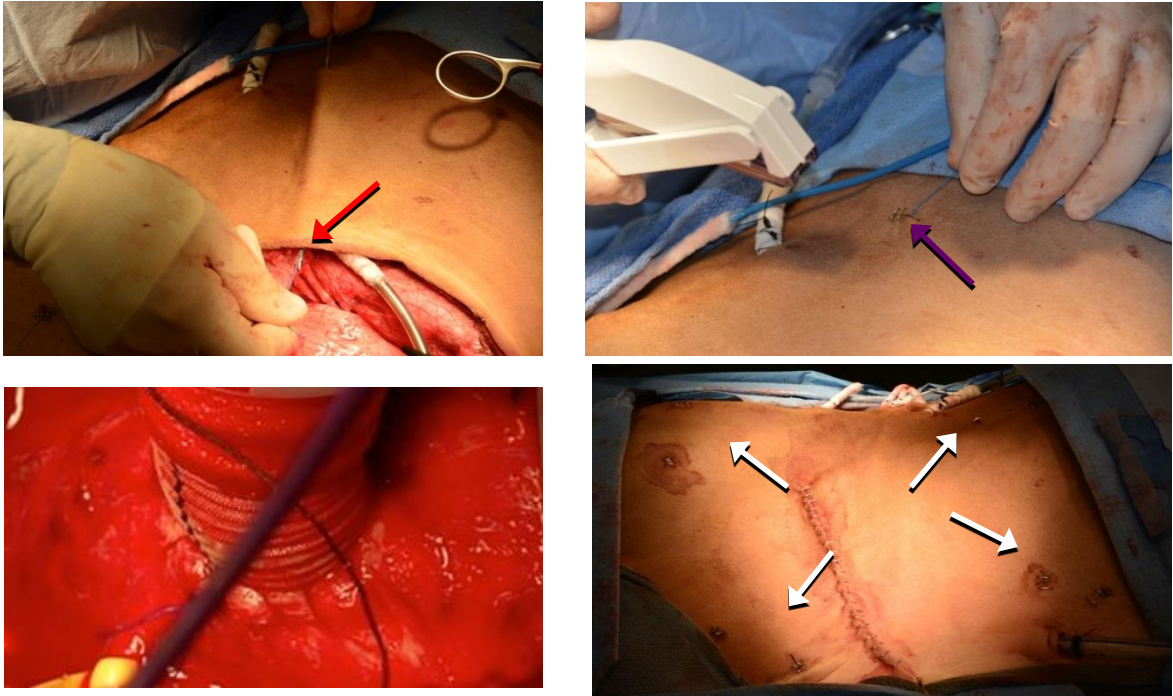


Figure 8. Tunneling of the subcutaneous ECG lead (red arrow, upper left). Surgical staples (purple arrow) being placed for subcutaneous ECG lead fixation and to serve as a landmark for evaluating lead migration at necropsy (upper right). Aortic anastomosis (lower left) and location of ECG leads (white arrows, lower right).

Post-Operative Procedure

After CPD implant procedure, the calves were transferred to the post-operative care area and monitored continuously for 30 days or until the study was terminated under order of the attending veterinarian for pain management reasons. Following admission to post-operative recovery, subcutaneous and epicardial waveforms were recorded for 30 seconds at hourly intervals. Both

signals were conditioned using the CPD driver (iPulse, Abiomed, Danvers, MA). The waveforms were collected at 400 Hz (National Instruments, AT-MIO-16E-10, Austin, TX), and were filtered using a clinical standard 60 Hz notch filter (Frequency Devices, Ottawa IL). All waveforms were visualized and recorded using a custom, good laboratory practice (GLP) approved data acquisition system (DAQ).

Euthanasia Procedures

After 30 days of device usage and data acquisition, calves were examined under fluoroscopy, heparinized, and subsequently euthanized with a bolus of Beuthanasia solution (30ml I.V.) followed by two boluses of KCl (30mEq). This procedure is in accordance with the recommended practices of the 2007 American Veterinary Medical Association Guidelines on Euthanasia. The calves were immediately exsanguinated and a full necropsy was performed for each calf to detect the occurrence of internal adverse events or infection. To quantify lead migration and lead damage, the lead sensing ends were visually compared to their placement staples using a metric ruler and the difference was recorded. Photographic documentation of lead migration was captured (Figure 9). The veterinarian completed a gross examination to detect external adverse events.

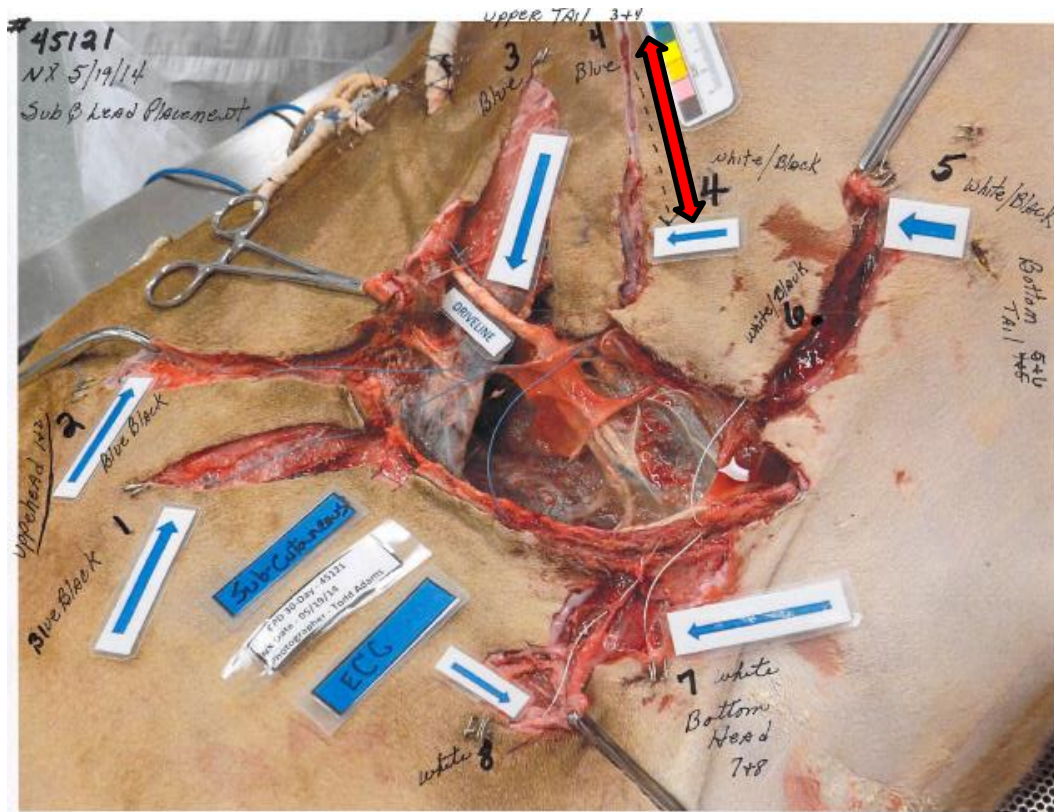


Figure 9. Photograph of subcutaneous lead migration (red arrow) in calves at the termination of the study. Staples were placed on the skin upon lead implantation to be used as a reference for original lead placement. Only one lead was found to migrate more than 0.5cm as shown above.

Post-Processing

Post-euthanasia, subcutaneous and epicardial ECG waveforms from the collected data epochs were analyzed to compare detection rates using computer software (MATLAB, The Mathworks, Natick, MA). For R-wave comparison, waveforms were analyzed on a beat-to-beat basis using custom m-files written in MATLAB (Mathworks, Natick MA). The original scripts published by Warren, et al. required input of the epicardial ECG waveform along with three separate bi-polar

subcutaneous ECG waveforms [4]. During this study, a total of two ECG waveforms were saved (1 epicardial, 1 subcutaneous). Therefore, the scripts were modified to allow for the difference in signal format. Once both ECG waveforms were loaded into MATLAB, every subcutaneous (test) R-wave or lack thereof was compared to the epicardial (control) R-wave in each data epoch and classified as a true positive, false positive, or false negative R-wave. The same R-wave detection mechanism used in the CPD driver was used when detecting and comparing R-waves for both signals. The first function of this program aligns the first R-waves of the subcutaneous and epicardial waveforms to account for the difference in lead lengths. Although the time difference between peaks in each waveform is small, any misalignment could potentially lead to a hindrance in R-wave detection. To do this, the program searches each waveform for the first local maximum indicated by user input of a specific time window. Once the waveforms' first QRS peaks are identified they are aligned by splicing data points from the beginning of the subcutaneous waveform and truncating the end of the epicardial waveform. Next, a 1-50 Hz (N=700) finite impulse response band-pass filter was implemented for optimal detection and to eliminate baseline drift.

For R-wave comparison, the signals were derived to detect major differences in slope before and after the R-wave. The program was given a threshold for the first three R-waves and then a bootlegging mechanism propagated the detection using a percentage of the average of the last three R-wave thresholds. If the QRS complex was detected in both waveforms, the signal

was classified as true positive. A maximum time difference of 150 ms between epicardial and subcutaneous ECG was used to calculate true positive in accordance with ANSI/AAMI EC 57 standard. If the QRS was detected in the epicardial waveform, but not in the subcutaneous waveform it was classified as a false negative. If the QRS was detected in the subcutaneous waveform, but not in the epicardial waveform it was classified as a false positive. These classifications were used to calculate Positive Predictive Value (1) and Sensitivity (2). If a signal was not collected or there was electrical noise during data capture, that data epoch was not used in the average calculations.

$$\text{Positive Predictive Value (PPV)} = \frac{\textit{True Positive}}{\textit{True Positive} + \textit{False Positive}} \quad (1)$$

$$\text{Sensitivity} = \frac{\textit{True Positive}}{\textit{True Positive} + \textit{False Negative}} \quad (2)$$

PPV is a representation of type I error and sensitivity is a representation of type II error. Of the two types of error, type I error is more detrimental for counterpulsation therapy. If a false R-wave is falsely detected (type I error), it would cause an unsynchronized filling and ejection which may increase LVEW and diminish coronary perfusion and advance the state of heart failure. If an R-wave is not detected (Type II error), the device would not fill or eject for that heart beat and would not adversely affect the baseline hemodynamics. If R-waves are not detected (Type II error) for a prolonged period, the CPD driver would switch to a

temporary 'wash mode', and slowly wash blood in and out of its 30 ml chamber to protect the patient from thrombosis.

RESULTS

Out of the six calves that survived IHF induction, one died after CPD implantation before any data could be acquired, and was therefore not included in this summary. From the remaining five calves, 791 data epochs were measured and recorded for chronic IHF calves (n=4) and control (n=1). Subcutaneous leads provided 98.8% PPV and 98.8% sensitivity when compared to epicardial leads (Table 2).

| Calf | Length of Study | Data Epochs | Total Heart Beats | PPV | Sensitivity |
|--------|-----------------|-------------|-------------------|---------------|---------------|
| 1 | 30-day | 347 | 18975 | 0.994 ± 0.023 | 0.985 ± 0.047 |
| 2 | 10-day | 71 | 4429 | 0.996 ± 0.014 | 0.988 ± 0.034 |
| 3 | 6-day | 27 | 1371 | 0.978 ± 0.041 | 0.958 ± 0.074 |
| 4 | 30-day | 289 | 15168 | 0.985 ± 0.030 | 0.995 ± 0.021 |
| 5 | 30-day | 57 | 2829 | 0.967 ± 0.048 | 0.981 ± 0.046 |
| Totals | Chronic | 791 | 42772 | 0.988 ± 0.030 | 0.988 ± 0.040 |

Table 2. Positive predictive value (PPV) and sensitivity of R-wave detection calculated from subcutaneous ECG recordings. Each data epoch consists of 30 seconds of ECG signaling. Values are listed as mean ± standard error.

An example of acquired subcutaneous and epicardial waveforms are shown in Figure 10. One chronic calf was euthanized ten days after CPD implant at the discretion of the attending veterinarian for pain management and another

died from heart failure symptoms six days after CPD implant. The accumulated epochs offered a total of 416.5 minutes of recorded ECG waveforms.

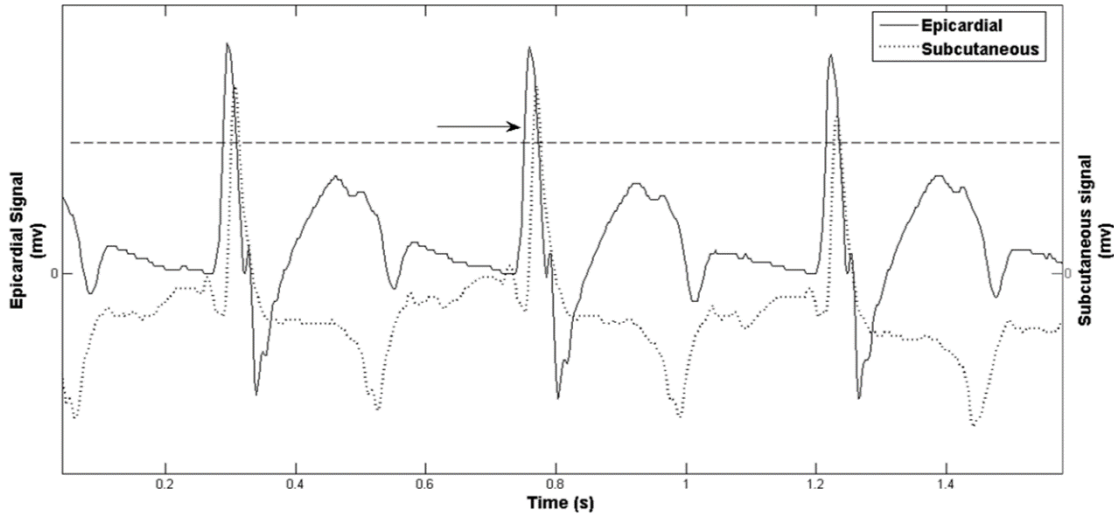


Figure 10. Subcutaneous (dashed line) ECG demonstrated a 98.9% PPV and 98.9% sensitivity for counterpulsation timing compared to epicardial (solid line) ECG leads.

Lead migration (n=1, >0.05 cm) and lead fracture (n=1) were only observed in two out of 40 leads and did not adversely impact triggering efficacy.

DISCUSSION

Upon inspection of the recorded ECG signals, electrical noise was found. However, if a QRS complex could be seen visually, then custom m-files were used to compare R-wave detection rates. After excluding incomplete data epochs (missing epicardial waveforms, missing subcutaneous waveforms, or

indiscernible waveforms), subcutaneous ECG leads were found to have a 98.8% PPV and 98.8% sensitivity. False positive and false negative beats were calculated in comparison to the epicardial lead ECG signal and not the actual myocardial contraction. Thus, even if the subcutaneous lead correctly picked up the ECG signal but epicardial lead was erroneous and vice versa, it still registered as a false positive and false negative, reducing PPV and sensitivity values for the subcutaneous leads. Despite these limitations, the performance of the epicardial ECG leads exceeded the design specifications of 95% PPV and 95% sensitivity. These results demonstrate that the subcutaneous leads are equivalent to epicardial leads for counterpulsation device triggering and R-wave detection. Noise and motion artifacts don't significantly alter the detection rate.

Two of 40 subcutaneous leads had a migration or fracture. However, in the case of a loss in signal or reduced signal strength, the controller automatically switches to another lead pair for ECG signaling. This provides redundancy and the detection algorithm embedded in the CPD driver automatically picks the best ECG signal available for device timing [39]. Therefore, lead migration and fracture did not diminish the efficacy of the CPD due to the redundant design.

Adverse events were reported by the veterinarian throughout the duration of the study and upon termination of the study (necropsy). There were no hemolysis, thrombus formation in device, graft or end organs, or vascular injury

events associated with the CPD. The aortic cannulation was patent throughout the duration of the study. A limitation of the study was that the subcutaneous and epicardial signals were first input into the CPD driver for processing, filtering, and amplification before being output into the GLP compliant DAQ which removes the ability to analyze raw signals, and increases the opportunity for noise to distort the saved signals.

CHAPTER 3 – ACUTE *in-vivo* ANIMAL STUDY

INTRODUCTION

The two objectives of this study were to 1) demonstrate acute subcutaneous lead efficacy in providing reliable cardiac signaling for proper device triggering and 2) demonstrate feasibility of aortic CPD cannulation under pharmacologically induced conditions. The outline of the study is shown in Table 3.

| Animal ID | Procedure Date | Necropsy Date | Reason for Termination |
|-----------|----------------|---------------|------------------------|
| 1 | 12/6/13 | 12/6/13 | full term |
| 2 | 12/9/13 | 12/9/13 | full term |
| 3 | 3/18/14 | 3/18/14 | full term |
| 4 | 5/6/14 | 5/6/14 | died during surgery |
| 5 | 3/14/14 | 3/14/14 | full term |

Table 3. Summary of acute calves used for ECG lead testing and hemodynamic testing.

For this study, an acute, non-HF model was used (n=5). CPD, subcutaneous leads, and epicardial leads were implanted along with pressure and flow sensors for hemodynamic waveform acquisition. ECG and hemodynamic waveforms were simultaneously collected during normal and pharmacologically induced hypertension, hypotension, and heart failure test conditions. At the end of each experiment, the animals were euthanized.

MATERIALS AND METHODS

Following the CPD implantation procedures outlined previously (Chapter 3), 14 lines of instrumentation were implanted before the CPD was implanted in preparation for hemodynamic testing. Specifically, fluid-filled catheters were inserted into the left carotid artery and left jugular vein to acquire arterial pressure (ArtP) and central venous pressure (CVP), respectively. High fidelity pressure catheters (Millar Instruments, Houston, TX) were used to measure left atrial pressure (LAP) and aortic pressure (AoP). Left ventricular pressure (LVP) and left ventricular volumes (LVVol) were collected using a volume conductance catheter (Transonic Systems Inc., Ithaca, NY). Transit time flow probes (Transonic Systems Inc., Ithaca NY) of varying sizes were used to obtain flow waveforms. Flow probes were covered with transonic signal enhancement liquid and then wrapped around the left carotid artery (CdAF), left main coronary artery (CAF), aorta proximally to the heart (AOFp), aorta distally from the heart (AOFd), and pulmonary artery (PAF). The electrical cardiac signals (subcutaneous, epicardial, and surface) were also routed to the DAQ to be acquired for future use. External ECG leads were used only for intra-operative monitoring. All lines of instrumentation except surface ECG electrodes were tunneled out of the lower thoracic cavity of each bovine and connected to the custom GLP DAQ. Both of the implanted ECG lead systems were routed directly into the CPD driver to be used for synchronized device triggering. From there, the filtered, amplified ECG waveforms were sent to the DAQ to be collected.

Hemodynamic waveforms were captured and recorded during: (1) normal (mean arterial pressure between 65 - 120 mmHg); (2) hypotension (mean arterial pressure < 65 mmHg induced by Nitroprusside); (3) hypertension (mean arterial pressure > 120 mmHg induced by Phenylephrine); and (4) heart failure (a 50% decrease in PAF induced by Esmolol). All conditions were allowed to normalize for 15 minutes before data was acquired. In each condition, 30 second data sets were taken of no pump support, 1:2 support, and 1:1 support. Experiments ended with euthanasia and a full necropsy to detect adverse events totaling experiment time from 6 to 8 hours. Complete photographic documentation of adverse events was recorded.

After the calf was euthanized, the Millar catheters and the Transonic Systems Inc. pressure-volume catheters were calibrated using a sealed pressure chamber at -5mmHg, 50mmHg, 100mmHg, and 150mmHg. The Transonic flow probes were calibrated electronically in a stagnant bowl of saline at 0 and 1 Volts.

All waveforms were saved using the GLP compliant DAQ system. For ECG waveforms, post-processing was performed as described in chronic experiments (Chapter 3). For hemodynamic waveforms, post-processing was performed using computer software (MATLAB, The Mathworks, Natick, MA). Specifically, Hemodynamic Evaluation and Assessment Tool (HEART) was used to determine hemodynamic efficacy [40]. Blood pressure and flow waveforms

were input into the program to calculate heart rate (HR), stroke volume (SV), cardiac output (CO), mean coronary artery flow (CAFm), left ventricular peak systolic pressure (LVPSP), left ventricular end diastolic pressure (LVEDP), left atrial pressure (LAP), left ventricular end systolic volume (LVVes), left ventricular end diastolic volume (LVVed), LVEW, mean aortic pressure (AoPm), and aortic pulse pressure (AoP pulse). All parameters were averaged to establish one mean value and were subsequently analyzed in Minitab (Minitab Inc., State College, PA). Two-tailed paired t-tests were used to compare no support to 1:1 support at each induced pharmacologic condition. A P-value of 0.05 or a confidence interval of 95% was considered statistically significance.

RESULTS

Out of the four calves that survived cardiac surgery, only two had epicardial and subcutaneous waveforms with distinguishable QRS complexes. 42 data epochs were measured and recorded in these two calves. The subcutaneous leads had a 99.7% PPV and 100% sensitivity compared to epicardial leads (Table 4).

The CPD cannulated to the aorta diminished left ventricular (LV) external work (up to 31%), LV end diastolic volume by 31ml (247ml vs 278.2ml at baseline) and end systolic volumes by 42ml (139.2ml vs 181.2ml at baseline) during pharmacologically induced heart failure (HF). Cardiac output, aortic mean,

pulse pressures, and mean coronary artery flow were augmented by up to 17.9%, 13.0%, 62.3%, and 52.4%, respectively (Table 5). The hemodynamic benefits of the CPD were not as profound for normal, hypotension and hypertension test conditions compared to HF test condition.

| Calf | Length of Study | Data Epochs | Total Heart Beats | PPV | Sensitivity |
|--------|-----------------|-------------|-------------------|---------------|---------------|
| 1 | 1-day | 16 | 697 | 0.993 ± 0.018 | 1.000 ± 0.000 |
| 2 | 1-day | 23 | 1145 | 1.000 ± 0.000 | 1.000 ± 0.000 |
| Totals | Acute | 39 | 1842 | 0.997 ± 0.099 | 1.000 ± 0.000 |

Table 4: Positive predictive value (PPV) and sensitivity of R-wave detection calculated from intra-operative subcutaneous ECG recordings. Each data epoch consists of 30 seconds of ECG signaling. Values are listed as mean ± standard error.

| Condition and Support | HR (bpm) | CO (L/min) | CAFM (mL/min) | LVPSP (mm Hg) | LVEDP (mm Hg) | LAP (mm Hg) | LVEs (ml) | LVEd (ml) | LV EW (mmHg-ml) | AoP mean (mm Hg) | AoP pulse (mm Hg) |
|-----------------------|----------|------------|---------------|---------------|---------------|-------------|------------|------------|-----------------|------------------|-------------------|
| Heart Failure | | | | | | | | | | | |
| Baseline | 84±6 | 4.5±0.2 | 48±27 | 48.1±4.9 | 15.9±3.5 | 14.0±1.2 | 181.2±29.1 | 278.0±21.0 | 1434±664 | 30.9±2.9 | 23.4±5.6 |
| 1:2 | 88±9 | 5.7±0.4 | 53±9 | 52.2±4.5 | 18.6±1.0 | 14.1±1.4 | 159.1±24.2 | 274.3±25.2 | 1978±341 | 35.4±5.7 | 31.8±10.4 |
| 1:1 | 87±5 | 5.3±0.3 | 73±12 | 47.4±3.6 | 16.6±1.7 | 13.5±0.6 | 139.2±54.4 | 247.2±2.4 | 987±440 | 34.9±3.8 | 38.0±7.2 |
| Hypotension | | | | | | | | | | | |
| Baseline | 109±15 | 8.5±0.9 | 118±12 | 81.1±10.3 | 10.3±2.1 | 8.7±1.1 | 128.4±24.2 | 228.6±23.3 | 4640±592 | 44.6±1.6 | 33.8±2.7 |
| 1:2 | 108±13 | 8.6±1.0 | 102±10 | 85.1±13.8 | 13.6±1.7 | 8.6±0.9 | 125.5±19.4 | 262.1±51.1 | 4842±467 | 45.0±1.6 | 44.1±8.1 |
| 1:1 | 101±7 | 8.5±0.9 | 102±8 | 67.7±2.1 | 12.5±0.9 | 8.3±1.0 | 123.9±19.2 | 260.4±50.9 | 3394±1247 | 43.7±1.5 | 42.3±5.7 |
| Hypertension | | | | | | | | | | | |
| Baseline | 96±5 | 13.2±1.3 | 222±33 | 178.8±30.9 | 16.0±0.6 | 9.8±0.7 | 94.6±52.3 | 297.5±85.5 | 18147±1413 | 129.3±6.4 | 37.7±5.7 |
| 1:2 | 87±5 | 12.1±1.4 | 199±30 | 169.2±16.8 | 15.3±1.6 | 9.6±0.5 | 91.8±56.5 | 207.9±73.2 | 18172±145 | 124.4±8.1 | 42.3±8.6 |
| 1:1 | 98±9 | 12.5±1.0 | 234±20 | 188.4±25.0 | 15.9±1.4 | 10.0±0.4 | 115.6±56.5 | 293.0±83.2 | 18191±1287 | 140.4±18.9 | 50.4±4.6 |
| Normal | | | | | | | | | | | |
| Baseline | 91±3 | 11.7±0.0 | 131±17 | 106.7±10.8 | 13.0±1.0 | 8.6±1.6 | 81.3±20.4 | 243.1±19.1 | 10810±1093 | 79.1±6.2 | 33.1±3.5 |
| 1:2 | 93±5 | 11.6±0.4 | 130±20 | 107.9±11.9 | 12.2±0.9 | 8.4±0.9 | 64.2±44.4 | 224.7±2.1 | 10606±946 | 82.3±5.9 | 39.0±4.7 |
| 1:1 | 92±5 | 11.6±0.4 | 122±18 | 102.1±10.7 | 12.8±1.8 | 8.8±0.7 | 49.3±55.3 | 217.0±0.3 | 9859±630 | 78.1±3.5 | 41.9±5.2 |

Table 5. Hemodynamic parameters during acute counterpulsation therapy with the CPD device cannulated to the aorta in calves with pharmacologically induced hypertension, hypotension, and heart failure. HR, heart rate; SV, stroke volume; CO, cardiac output; CAFm, mean coronary artery flow; LVPSP, left ventricular peak systolic pressure; LVEDP, left ventricular end diastolic pressure; LAP, left atrial pressure; LVEs, left ventricular end systolic volume; LVEd, left ventricular end diastolic volume; LVEW, left ventricular external work; AoP mean, mean aortic pressure; AoP pulse, aortic pulse pressure

Pressure-volume loop figures represent the LVEW and ventricular hemodynamic conditions during heart failure, hypertension, hypotension, and normal test conditions (Figures 11, 13, 15, 17). LVP, AoP, and CAF waveforms demonstrate changes in perfusion and pulsatility between each test condition (Figures 12, 14, 16, 18). The hemodynamic benefits from heart failure show the most significant improvement with CPD support (Figures 11-12). CPD support diminished LVEW, left ventricular end systolic and end diastolic volumes, and augmented coronary perfusion, aortic pressures and aortic pulsatility during heart failure (Figures 11-12). The hemodynamic benefits of CPD support were not statistically discernable from baseline values.

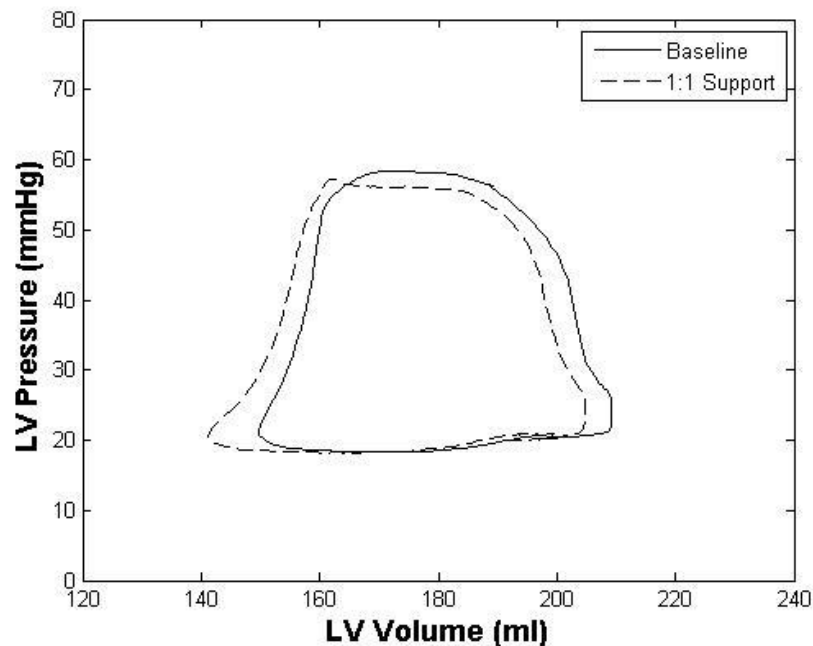


Figure 11. Pressure-volume loops obtained from an acute animal study at baseline (solid, no CPD support), and 1:1 CPD support (dashed) during a pharmacologically induced heart failure test condition. These PV loops demonstrate the reduction in LVEW, end systolic volume, and end diastolic volume with CPD support.

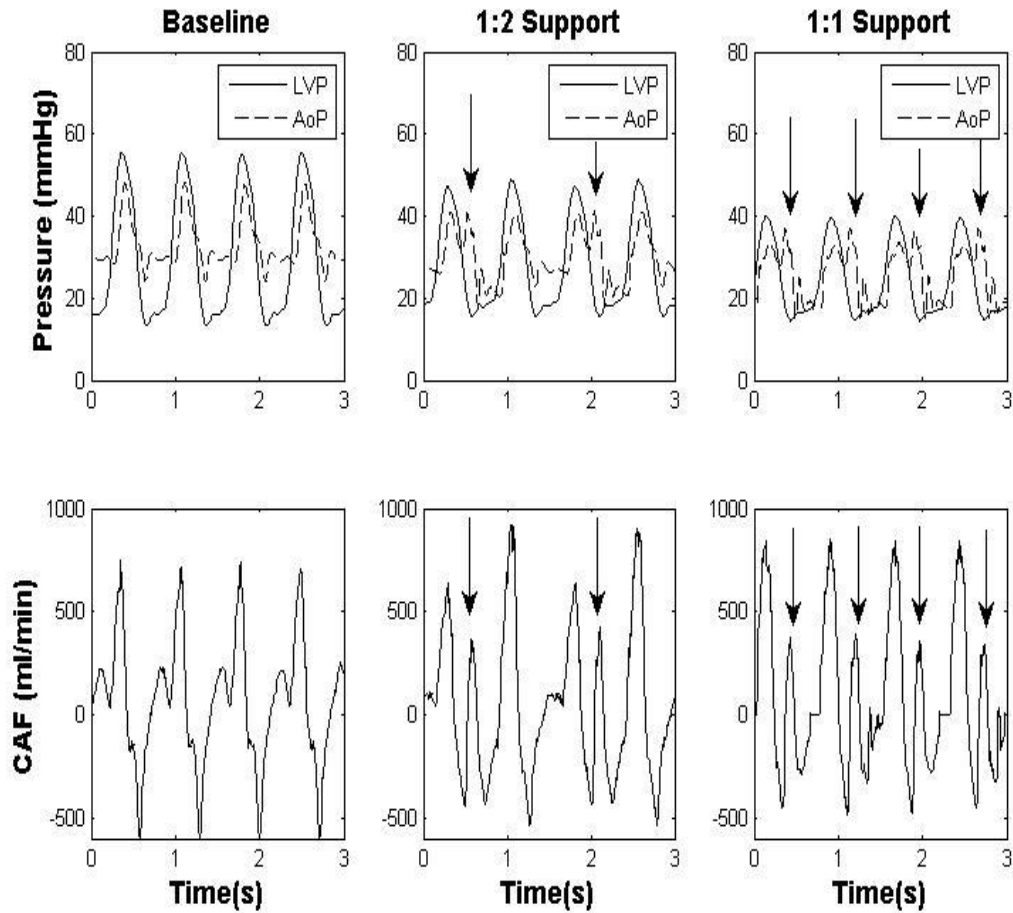


Figure 12. Aortic pressure (AoP, dotted), LV pressure (LVP, solid), and coronary artery flow waveforms obtained during a pharmacologically induced heart failure test condition at baseline (no CPD support), 1:2 support, and 1:1 support. These waveforms indicate a lower ventricular ejection pressure and higher aortic diastolic pressures (arrows, top) and coronary artery flow (arrows, bottom) during counterpulsation support.

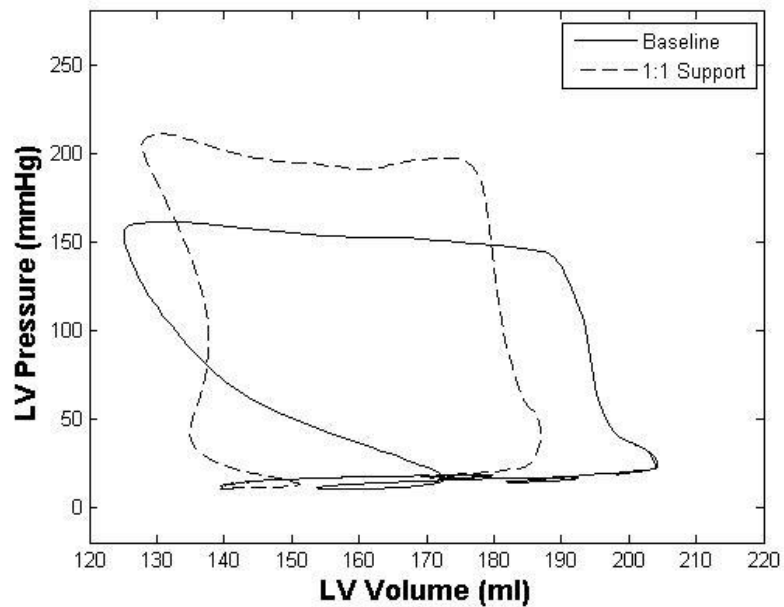


Figure 13. Pressure-volume loops obtained at baseline (solid, no CPD support) and 1:1 CPD support (dashed) during a pharmacologically induced hypertension test condition. The hemodynamic benefits such as reductions in LVEW, end systolic volume, and end diastolic volume are not evident compared to the heart failure test condition as the stroke volume of the native heart (135 ml) was much greater than the counterpulsation device volume (30 ml).

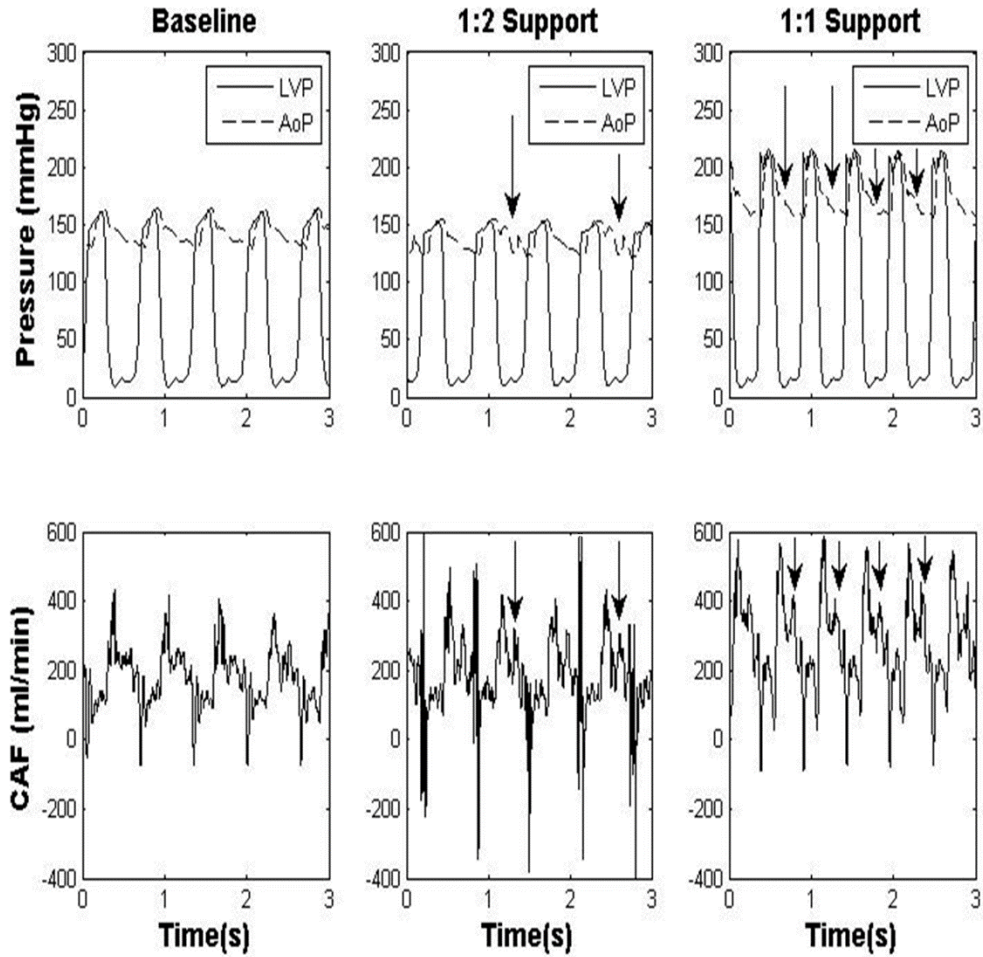


Figure 14. Aortic pressure (AoP, dotted), LV pressure (LVP, solid), and coronary artery flow waveforms obtained during a pharmacologically induced hypertension test condition at baseline (no CPD support), 1:2 support, and 1:1 support. The hemodynamic benefits such as lower ventricular ejection pressure and higher aortic diastolic pressures (arrows, top) and coronary artery flow (arrows, bottom) are not evident compared to the heart failure test condition as the stroke volume of the native heart (135 ml) was much greater than the counterpulsation device volume (30 ml).

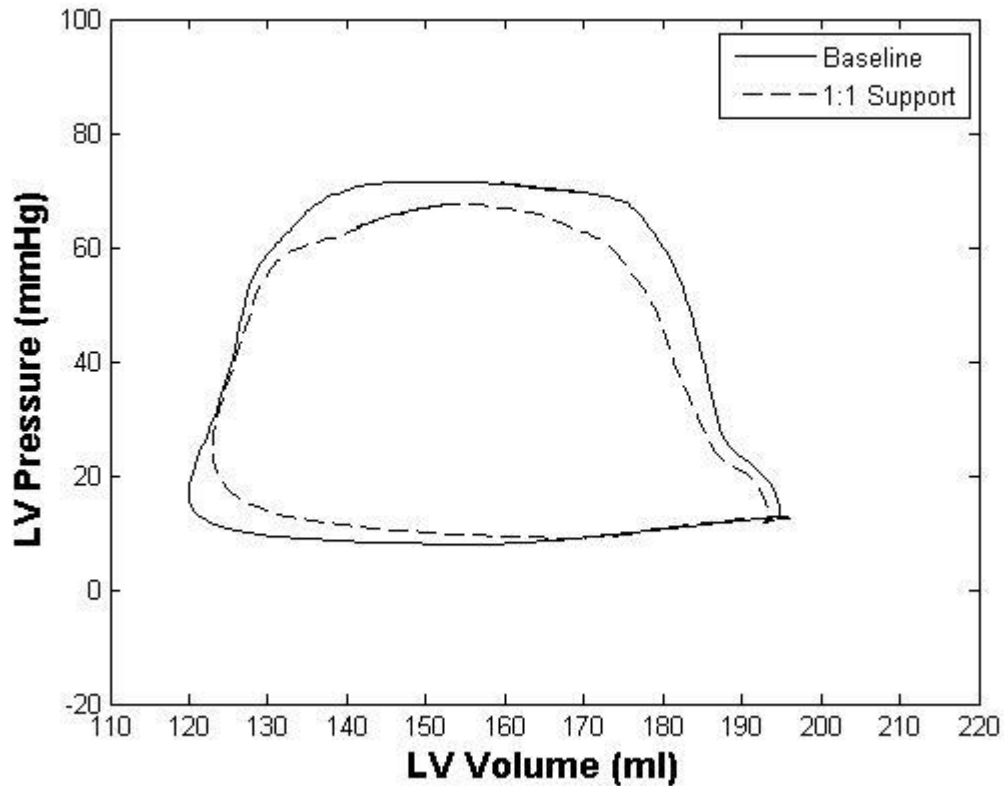


Figure 15. Pressure-volume loops obtained at baseline (solid, no CPD support), and 1:1 CPD support (dashed) during a pharmacologically induced hypotension test condition. The hemodynamic benefits such as reductions in LVEW, end systolic volume, and end diastolic volume are not evident compared to the heart failure test condition as the stroke volume of the native heart (82 ml) was much greater than the counterpulsation device volume (30 ml).

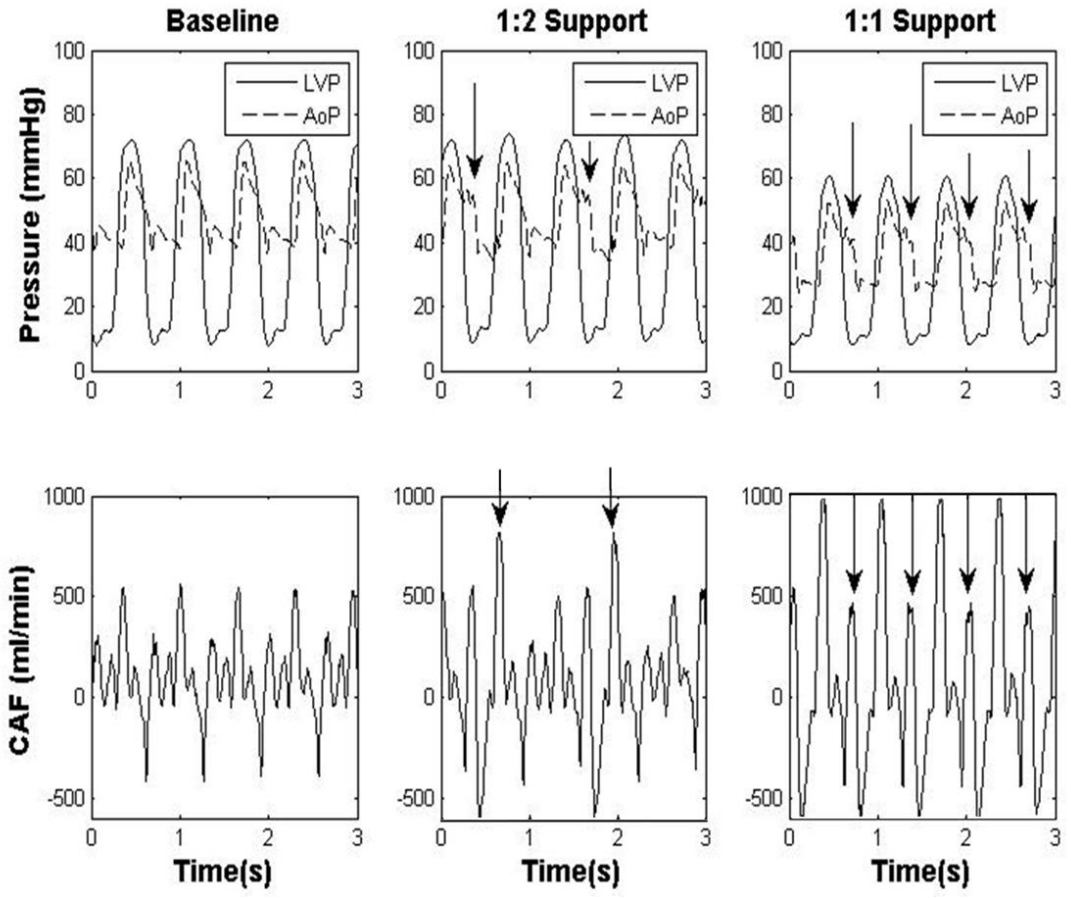


Figure 16. Aortic pressure (AoP, dotted), LV pressure (LVP, solid), and coronary artery flow waveforms obtained during a pharmacologically induced hypotension test condition at baseline (no CPD support), 1:2 support, and 1:1 support. These waveforms indicate a lower ventricular ejection pressure and higher aortic diastolic pressures (arrows, top) and coronary artery flow (arrows, bottom) during counterpulsation support.

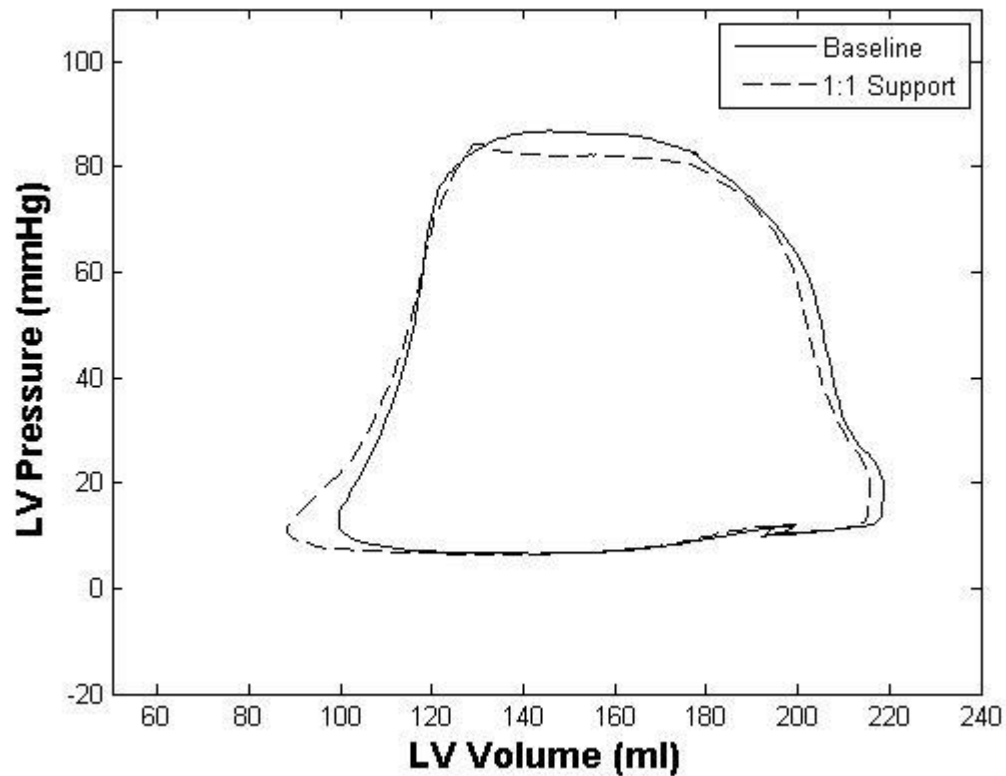


Figure 17. Pressure-volume loops at baseline (solid, no CPD support), and 1:1 CPD support (dashed) during a normal test condition. The hemodynamic benefits such as reductions in LVEW, end systolic volume, and end diastolic volume are not evident compared to the heart failure test condition as the stroke volume of the native heart (128 ml) was much greater than the counterpulsation device volume (30 ml).

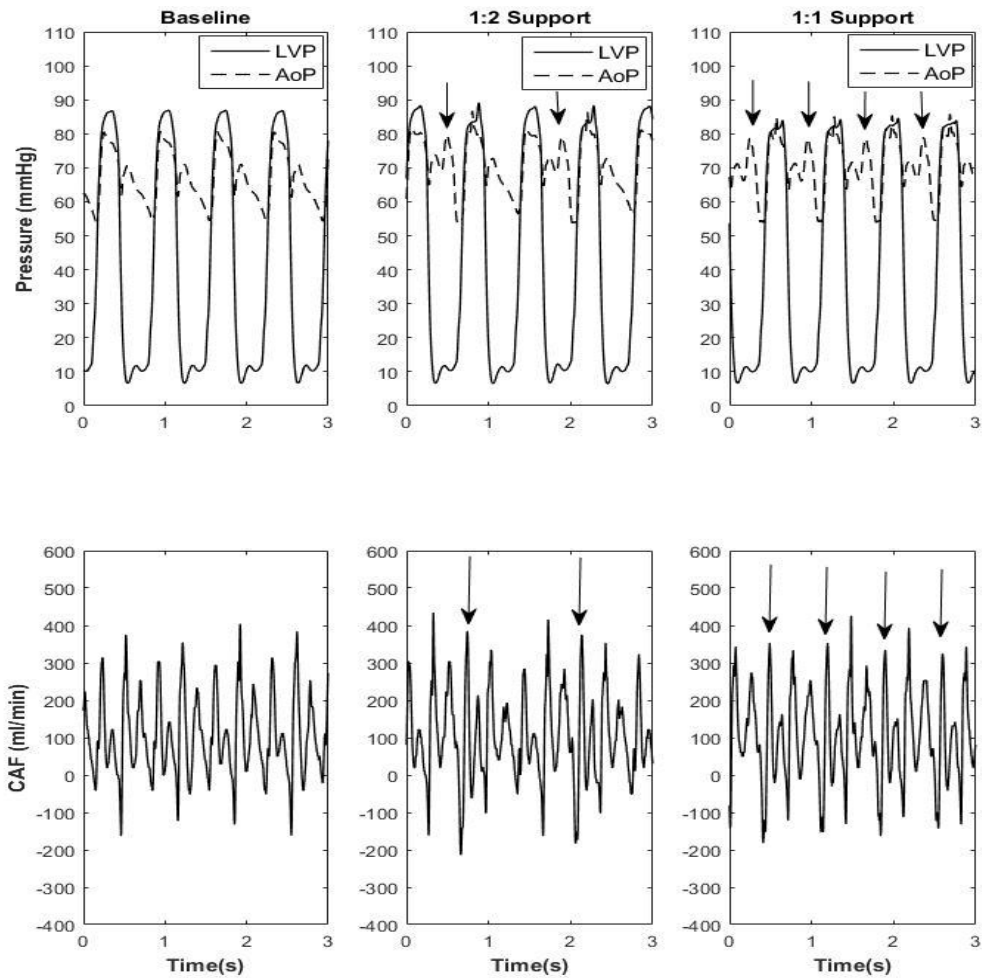


Figure 18. Aortic pressure (AoP, dotted), LV pressure (LVP, solid), and coronary artery flow waveforms obtained during a normal test condition at baseline (no CPD support), 1:2 support, and 1:1 support. Lower ventricular ejection pressure and higher aortic diastolic pressures (arrows, top) and coronary artery flow (arrows, bottom) during counterpulsation support are not as evident compared to the heart failure test condition as the stroke volume of the native heart (128 ml) was much greater than the counterpulsation device volume (30 ml).

DISCUSSION

The >99% PPV and sensitivity values demonstrated that the epicardial leads can adequately trigger the CPD during a wide range of physiologic conditions. Hemodynamically, cardiac output, coronary perfusion, aortic pressure, and aortic pulsatility showed an increasing trend and decreases were observed in end-systolic and end-diastolic left ventricular volumes and LVEW. The benefits of counterpulsation are most pronounced when counterpulsation device volume is similar to the stroke volume of the native heart and at low aortic compliances [41]. The hemodynamic waveforms from the animal study closely resembles counterpulsation waveform morphology observed clinically and in an earlier computer simulation study [42]. However, the hemodynamic benefits of CPD support was not evident at normal, hypertensive, and hypotensive conditions in the acute animal study as the stroke volume of the native heart (128, 135, and 82 ml respectively) was much greater than the counterpulsation device volume (30 ml). Further, the aortic compliance of a calf is significantly greater than that of a human with HF [41]. Due to these factors and low sample size (n=3), statistical significance could not be ascertained between baseline and 1:1 CPD support, but improving hemodynamic trends with CPD support demonstrate the feasibility of aortic cannulation. While aortic anastomosis would increase the invasiveness of device implantation in patients with small subclavian arteries, chronic counterpulsation may enable earlier intervention (Class III) and arrest the progression of HF.

The hemodynamic benefits provided by the CPD anastomosed to the aorta would be slightly higher than the benefits provided by the CPD anastomosed to the subclavian artery due to energy losses associated with the CPD being farther away from the aorta [21]. The hemodynamic parameters of the CPD anastomosed to the carotid artery in an acute bovine model (n=12) from an earlier study is presented in Table 6 [1].

| Physiological Condition | Support | | HR (bpm) | CO (L/min) | CAFdia (mL/min) | LVPSP (mm Hg) | LVPEDP (mm Hg) | LAP (mm Hg) |
|-------------------------|----------|-----|----------|------------|-----------------|---------------|----------------|-------------|
| Normal | Baseline | | 78 ± 4 | 8.0 ± 0.0 | 207 ± 46 | 103 ± 3 | 16 ± 2 | 14 ± 2 |
| Hypertension | Baseline | | 73 ± 4 | 8.1 ± 0.5 | 285 ± 43 | 138 ± 3 | 19 ± 2 | 14 ± 2 |
| | CPD | 1:2 | 77 ± 5 | 8.2 ± 0.6 | 305 ± 49 | 138 ± 3 | 19 ± 3 | 15 ± 2 |
| | | 1:1 | 76 ± 4 | 8.2 ± 0.6 | 314 ± 49 | 137 ± 3 | 19 ± 2 | 14 ± 2 |
| Hypotension | Baseline | | 70 ± 3 | 6.8 ± 0.5 | 141 ± 33 | 77 ± 2 | 11 ± 1 | 9 ± 1 |
| | CPD | 1:2 | 72 ± 3 | 6.8 ± 0.7 | 155 ± 33 | 76 ± 2 | 10 ± 1 | 9 ± 1 |
| | | 1:1 | 71 ± 3 | 6.8 ± 0.6 | 173 ± 43 | 74 ± 2 | 10 ± 1 | 8 ± 1 |
| Heart Failure | Baseline | | 66 ± 3 | 6.0 ± 0.3 | 139 ± 35 | 89 ± 5 | 22 ± 1 | 15 ± 1 |
| Failure | CPD | 1:2 | 67 ± 3 | 6.2 ± 0.3 | 153 ± 36 | 88 ± 5 | 22 ± 1 | 16 ± 1 |
| | | 1:1 | 67 ± 3 | 6.1 ± .03 | 159 ± 37 | 84 ± 4 | 21 ± 1 | 15 ± 1 |

TABLE 6. Hemodynamic parameters during acute counterpulsation therapy with the CPD cannulated to carotid artery in calves with pharmacologically induced hypertension, hypotension, and heart failure [1].

A limitation of the study is that the hemodynamic effects were observed under pharmacologically induced, acute conditions. Thus, the state of the animal was never completely stable due to the half-life of drugs. Chronic pathologies or a significantly higher sample size (n=10-12) may be required for demonstrating statistically significant hemodynamic benefit.

CHAPTER 4 - CONCLUSION

This study demonstrates the long-term efficacy of using subcutaneous leads to provide an accurate, reliable ECG waveform for R-wave detection to trigger counterpulsation devices shown by 98.9% PPV and 98.9% sensitivity for all test conditions. Since the adverse events associated with lead migration and lead fracture didn't impact device triggering, use of subcutaneous leads in future clinical therapies is promising. Additionally, this study demonstrates the feasibility of aortic cannulation for patients with small subclavian arteries.

CHAPTER 5 – LIST OF REFERENCES

1. Bartoli, C.R., et al., *A novel subcutaneous counterpulsation device: acute hemodynamic efficacy during pharmacologically induced hypertension, hypotension, and heart failure*. *Artif Organs*, 2010. **34**(7): p. 537-45.
2. Company, B.W.A.B.H., *Abiomed Announces Symphony, an Implantable Synchronized Heart Pump*. 2011, AHA Scientific Sessions.
3. Giridharan, G.A., et al., *Predicted hemodynamic benefits of counterpulsation therapy using a superficial surgical approach*. *Asaio j*, 2006. **52**(1): p. 39-46.
4. Warren, S., et al., *Feasibility of Subcutaneous ECG Leads for Synchronized Timing of a Counterpulsation Device*. *Cardiovascular Engineering and Technology*, 2011. **3**(1): p. 17-25.
5. Mozaffarian, D., et al., *Heart disease and stroke statistics--2015 update: a report from the American Heart Association*. *Circulation*, 2015. **131**(4): p. e29-322.
6. Wilson, K.B., *Health Care Costs 101*. California Healthcare Foundation, 2012.
7. Muntwyler, J., et al., *One-year mortality among unselected outpatients with heart failure*. *Eur Heart J*, 2002. **23**(23): p. 1861-6.
8. Pitt, B., et al., *The effect of spironolactone on morbidity and mortality in patients with severe heart failure. Randomized Aldactone Evaluation Study Investigators*. *N Engl J Med*, 1999. **341**(10): p. 709-17.
9. *e-Statistics Report on Transplant, Waiting List and Donor Statistics, in 2012 Summary Statistics, January 1 to December 31st, 2012*. . Canadian Institute for Health Information., 2008.
10. Koenig, S.C., et al., *Acute hemodynamic efficacy of a 32-ml subcutaneous counterpulsation device in a calf model of diminished cardiac function*. *Asaio j*, 2008. **54**(6): p. 578-84.
11. Moskowitz, A.J., E.A. Rose, and A.C. Gelijns, *The cost of long-term LVAD implantation*. *Ann Thorac Surg*, 2001. **71**(3 Suppl): p. S195-8; discussion S203-4.

12. Westaby, S. and P. Poole-Wilson, *Mechanical circulatory support in the UK*. Bmj, 2007. **334**(7586): p. 167-8.
13. *Costs Comparable Per Patient Between Impella and Intra-Aortic Balloon Pump at 90 Days*. Diagnostics and Interventional Cardiology.
14. Mozaffarian, D., et al., *Heart Disease and Stroke Statistics-2016 Update: A Report From the American Heart Association*. Circulation, 2016. **133**(4): p. e38-e360.
15. Kautzner, J., et al., *Technical aspects of implantation of LV lead for cardiac resynchronization therapy in chronic heart failure*. Pacing Clin Electrophysiol, 2004. **27**(6 Pt 1): p. 783-90.
16. Nanas, J.N. and S.D. Moulopoulos, *Counterpulsation: historical background, technical improvements, hemodynamic and metabolic effects*. Cardiology, 1994. **84**(3): p. 156-67.
17. Papaioannou, T.G. and C. Stefanadis, *Basic principles of the intraaortic balloon pump and mechanisms affecting its performance*. Asaio j, 2005. **51**(3): p. 296-300.
18. Bolooki, H., ed. , *Clinical Application of the Intra-Aortic Balloon Pump Futura*: New York, 1998(3rd edition).
19. Santa-Cruz, R.A., M.G. Cohen, and E.M. Ohman, *Aortic counterpulsation: a review of the hemodynamic effects and indications for use*. Catheter Cardiovasc Interv, 2006. **67**(1): p. 68-77.
20. Tsagalou, E.P., M.I. Anastasiou-Nana, and J.N. Nanas, *Intra-aortic balloon counterpulsation for the treatment of myocardial infarction complicated by acute severe heart failure*. Congest Heart Fail, 2009. **15**(1): p. 35-40.
21. Kolyva, C., et al., *Discerning aortic waves during intra-aortic balloon pumping and their relation to benefits of counterpulsation in humans*. J Appl Physiol (1985), 2009. **107**(5): p. 1497-503.
22. Scheidt, S., et al., *Intra-aortic balloon counterpulsation in cardiogenic shock. Report of a co-operative clinical trial*. N Engl J Med, 1973. **288**(19): p. 979-84.
23. Lefemine, A.A., et al., *Assisted circulation. III. The effect of synchronized arterial counterpulsation on myocardial oxygen consumption and coronary flow*. Am Heart J, 1962. **64**: p. 789-95.

24. Weiss, A.T., et al., *Regional and global left ventricular function during intra-aortic balloon counterpulsation in patients with acute myocardial infarction shock*. Am Heart J, 1984. **108**(2): p. 249-54.
25. Kern, M.J., et al., *Enhanced coronary blood flow velocity during intraaortic balloon counterpulsation in critically ill patients*. J Am Coll Cardiol, 1993. **21**(2): p. 359-68.
26. Ishihara, M., et al., *Effects of intraaortic balloon pumping on coronary hemodynamics after coronary angioplasty in patients with acute myocardial infarction*. Am Heart J, 1992. **124**(5): p. 1133-8.
27. Sun, J.C., R.K. Ghanta, and M.J. Davidson, *Highlights from the Transcatheter Cardiovascular Therapeutics Conference 2010: Washington, DC, September 21-25, 2010*. J Thorac Cardiovasc Surg, 2011. **142**(2): p. 468-71.
28. Sun, B., *Sunshine: Chronic Aortic Counterpulsation for Class III Heart Failure*. Transcatheter Cardiovascular Therapeutics, 2009.
29. Jeevanandam, V., et al., *Circulatory assistance with a permanent implantable IABP: initial human experience*. Circulation, 2002. **106**(12 Suppl 1): p. I183-8.
30. Fotuhi, P., et al., *R-wave detection by subcutaneous ECG. Possible use for analyzing R-R variability*. Ann Noninvasive Electrocardiol, 2001. **6**(1): p. 18-23.
31. Goldich, G., *Getting in sync with intra-aortic balloon pump therapy*. Nursing, 2011. **41 Suppl**: p. 10-3.
32. Lobodzinski, S.S. and M.M. Laks, *Comfortable textile-based electrocardiogram systems for very long-term monitoring*. Cardiol J, 2008. **15**(5): p. 477-80.
33. Schwartzman, D., et al., *Postoperative lead-related complications in patients with nonthoracotomy defibrillation lead systems*. J Am Coll Cardiol, 1995. **26**(3): p. 776-86.
34. Lawton, J.S., et al., *Sensing lead-related complications in patients with transvenous implantable cardioverter-defibrillators*. Am J Cardiol, 1996. **78**(6): p. 647-51.
35. Bardy, G.H., et al., *An entirely subcutaneous implantable cardioverter-defibrillator*. N Engl J Med, 2010. **363**(1): p. 36-44.
36. Andrew Grace, M.H., Warren Smith, Andrey Ardashev, Riccardo Cappato, Gust Bardy, *Evaluation of four distinct subcutaneous implantable*

- defibrillator (S-ICD®) lead systems in humans*. Heart Rhythm, 2006(3): p. S128-S129.
37. Juan F. Iglesias, D.G., Patrizio Pascale, Etienne Pruvot, *The implantable loop recorder: a critical review*. THE NEW DEVICE, 2009. **12**(3): p. 85-93.
 38. van Dam, P., et al., *Improving sensing and detection performance in subcutaneous monitors*. J Electrocardiol, 2009. **42**(6): p. 580-3.
 39. Hanlon-Pena, P.M. and S.J. Quaal, *Intra-aortic balloon pump timing: review of evidence supporting current practice*. Am J Crit Care, 2011. **20**(4): p. 323-33; quiz 334.
 40. Schroeder, M.J., et al., *HEART: an automated beat-to-beat cardiovascular analysis package using Matlab*. Comput Biol Med, 2004. **34**(5): p. 371-88.
 41. Koenig, S.C., et al., *Human, bovine and porcine systematic vascular input impedances are not equivalent: implications for device testing and xenotransplantation in heart failure*. J Heart Lung Transplant, 2008. **27**(12): p. 1340-7.
 42. Moulopoulos, S.D., *The limits of counterpulsation*. Int J Artif Organs, 1993. **16**(12): p. 803-5.

CHAPTER 6 – CURRICULUM VITAE

Stephen R. Carnahan
Graduate Student
Department of Bioengineering
University of Louisville
Louisville, Kentucky, USA
859-620-7296
srcarn02@icloud.com

Education

| | | |
|------|---------------------------|-----------------------------------------|
| 2016 | University of Louisville | Master of Engineering in Bioengineering |
| | GPA:----- | |
| 2015 | University of Louisville | Bachelor of Science in Bioengineering |
| | GPA: 3.76 | |
| 2011 | Walton Verona High School | High School Diploma |
| | GPA: 3.99 | |

Skills

- SolidWorks
- MATLAB
- Medical Devices
- Minitab
- Microsoft Office
- Anatomy and Physiology
- Statistics

Academic and Professional Experience

2013-2015 Three Academic Research Co-ops, Advanced Heart Failure Research at the Cardiovascular Innovation Institute (total: 1 year)

- Provided technical support for many grant and industry sponsored studies, including hemolysis testing for mechanical circulatory support devices.
- Assisted with instrumentation and data collection during open-heart surgery on calves.
- Observed VAD operations and collected myocardial samples for a tissue repository.
- Learned techniques related to instrument preparation & handling, inducing anesthesia, cardiac defibrillation, tissue procurement, tissue transportation & storage, administering regional blood flow microspheres, fluoroscopy exams, skin electrocautery & suturing, electrocardiograms, and hemodynamic exams.

2014 Part-time University of Louisville Employment, Tutoring

- Tasked with helping college students understand mathematical concepts and techniques from basic Algebra to Calculus II

2012-2013 Part-time University of Louisville Employment, Test Grader

- Tasked with grading Calculus tests and assessing depth of knowledge for Calculus I, II, and III material

2010-2011 Part-time Kroger Employee, Courtesy Clerk

- Tasked with pushing carts into the building and bagging customers' groceries

Academic and Professional Honors and Awards

| | |
|-----------------------------------------|-------------------------|
| Trustees Academic Scholarship | Fall 2011 - Spring 2016 |
| Dean's List | Spring 2014 |
| Dean's List | Fall 2011 - Spring 2013 |
| SPEED Alumni Award | Spring 2012 |
| SPEED Scholars Award | Fall 2011 - Spring 2012 |
| Dean's Scholar | Fall 2011 |
| Boy Scouts of America, Eagle Scout Rank | Summer 2009 |

Abstracts/Publications

1. **S Carnahan BS**, SC Koenig PhD, MA Sobieski RN CCP, E Schumer MD, G Monreal PhD, Y Choi BS, B Meuris MEng, L Tompkins MEng, MS Slaughter MD, GA Giridharan PhD. Efficacy of Subcutaneous ECG leads for Chronic Counterpulsation Therapy, 2016. (submitted)
2. Schumer E, Monreal G, **Carnahan S**, Sobieski M, Slaughter M. Venovenous Extracorporeal Membrane Oxygenation for Acute Respiratory Distress Syndrome, KMA, 2014. (published)
3. Schumer E, Monreal G, **Carnahan S**, Sobieski M, Slaughter M. Outcomes for Heart Transplantation in Patients Older than 64 at a Single-Center Institution, KMA, 2014. (published)

Extracurricular Activities, Volunteer Experience, Leadership Activities

| | |
|-------------------------------------------|------|
| 10-day Mission Trip to El Viejo Nicaragua | 2014 |
|-------------------------------------------|------|

- Palmetto Medical Initiative, based in Charleston, SC, is an organization that sends medical missionaries to underserved populations in Nicaragua and Uganda. The medical care team that I served with provided a range of services including the distribution of prescription drugs and providing patients with education, reading glasses, wound care, physical therapy, and Counseling. I secured over \$3000 in private funding for this mission. I spent most of my time on the trip distributing the pharmaceuticals and teaching our patients how to take each individual medicine, with the help of an interpreter.

Member of Biomedical Engineering Society 2011-2014

Campus Crusaders for Christ (CRU) 2011-2014

- Served as a worship leader during weekly meetings

Church Related Service 2001-present

- I have identified myself as a Christian all of my life; consequently, I would feel hypocritical if I didn't try to serve others the way Christ serves his people. Over the past few years, I have served people in the church and outside the church through various organizations. I have served them by giving my most valuable resources such as time and money to organizations such as HOPEMOB, Eyes That See, Habitat for Humanity (H4H), Palmetto Medical Initiative, etc. I have personally given my time to all of these different organizations, but outside of that I can say I live a life of servitude to the

people around me by watching their kids for them, leading them in worship during church, or feeding people that would otherwise go hungry.

Hobbies

2009-Present Snowboarding/Water Skiing

Snow sports and water sports have been a passion of mine ever since I was a little boy. However, seeing and riding the slopes of Kalispell, Montana is what really sparked a life-long passion in me to snowboard. There is nothing better than to fly down a mountain without another care in the world.

2007-Present Playing Piano/Singing

Every person that has ever heard me play piano has told me I have a gift for music. In fact, acceptance to the prestigious Governor's School of the Arts is primarily what allowed me to receive a Trustees Scholarship at the University of Louisville for my undergraduate and graduate degrees. In addition, I have accompanied for pay during various instrumental workshops and weddings. I have also volunteered my services to many non-profit organizations.

2011-Present Ultimate Frisbee

I have always had a strong body and when I came to college I found Ultimate Frisbee to be a very good fit for me. It is a highly competitive, safe, non-contact, and fun sport, but the best feature is how it keeps me fit from all of the running involved. Other Interests and Hobbies: Backpacking, camping, healthy living, reading, medicine, soccer, landscaping, and traveling.